Article:
Houghton, MJ, Kerimi, A, Tumova, S orcid.org/0000-0003-2044-4998 et al. (2 more authors) (2018) Quercetin preserves redox status and stimulates mitochondrial function in metabolically-stressed HepG2 cells. Free Radical Biology and Medicine, 129. pp. 296-309. ISSN 0891-5849

https://doi.org/10.1016/j.freeradbiomed.2018.09.037

Quercetin preserves redox status and stimulates mitochondrial function in metabolically-stressed HepG2 cells

Michael J. Houghton, Asimina Kerimi, Sarka Tumova, John P. Boyle, Gary Williamson

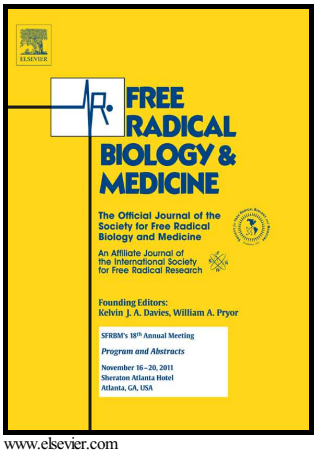

www.elsevier.com

PII: S0891-5849(18)31348-0
DOI: https://doi.org/10.1016/j.freeradbiomed.2018.09.037
Reference: FRB13939

To appear in: *Free Radical Biology and Medicine*

Received date: 3 August 2018
Revised date: 18 September 2018
Accepted date: 23 September 2018

Cite this article as: Michael J. Houghton, Asimina Kerimi, Sarka Tumova, John P. Boyle and Gary Williamson, Quercetin preserves redox status and stimulates mitochondrial function in metabolically-stressed HepG2 cells, *Free Radical Biology and Medicine,* https://doi.org/10.1016/j.freeradbiomed.2018.09.037

Quercetin preserves redox status and stimulates mitochondrial function in metabolically-stressed HepG2 cells.

Michael J. Houghton[a], Asimina Kerimi[a], Sarka Tumova[a], John P. Boyle[b], Gary Williamson[a,*]

[a]School of Food Science and Nutrition, Faculty of Maths and Physical Sciences, University of Leeds, Leeds, LS2 9JT, UK
[b]Leeds Institute of Cardiovascular and Metabolic Medicine, Faculty of Medicine and Health, University of Leeds, Leeds, LS2 9JT, UK

[*]Correspondence to: School of Food Science and Nutrition, Faculty of Maths and Physical Sciences, University of Leeds, Leeds, LS2 9JT, UK. g.williamson@leeds.ac.uk

Abstract

Hyperglycemia augments formation of intracellular reactive oxygen species (ROS) with associated mitochondrial damage and increased risk of insulin resistance in type 2 diabetes. We examined whether quercetin could reverse chronic high glucose-induced oxidative stress and mitochondrial dysfunction. Following long-term high glucose treatment, complex I activity was significantly decreased in isolated mitochondria from HepG2 cells. Quercetin dose-dependently recovered complex I activity and lowered cellular ROS generation under both high and normal glucose conditions. Respirometry studies showed that quercetin could counteract the detrimental increase in inner mitochondrial membrane proton leakage resulting from high glucose while it increased oxidative respiration, despite a decrease in electron transfer system (ETS) capacity, and lower non-ETS oxygen consumption. A quercetin-stimulated increase in cellular NAD^+/NADH was evident within 2 h and a two-fold increase in PGC-1α mRNA within 6 h, in both normal and high glucose conditions. A similar pattern was also found for the mRNA expression of the repulsive guidance molecule b (RGMB) and its long non-coding RNA (lncRNA) RGMB-AS1 with quercetin, indicating a potential change of the glycolytic phenotype and suppression of aberrant cellular growth which is characteristic of the HepG2 cells. Direct effects of quercetin on PGC-1α activity were minimal, as quercetin only weakly enhanced PGC-1α binding to PPARα in vitro at higher concentrations. Our results suggest that quercetin may protect mitochondrial function from high glucose-induced stress by increasing cellular NAD^+/NADH and activation of PGC-1α-mediated pathways. Lower ROS in combination with improved complex I activity and ETS coupling efficiency under conditions of amplified oxidative stress could reinforce mitochondrial integrity and improve redox status, beneficial in certain metabolic diseases.

Abbreviations

AmA – antimycin A; AMPK – adenosine monophosphate-activated protein kinase; CoQ – coenzyme Q_{10}; DCF – 2′,7′-dichlorofluorescin; DCFH-DA – 2′,7′-dichlorofluorescin diacetate; ddPCR – droplet digital PCR; ETS – electron transfer system; FBS – fetal bovine serum; FCCP – carbonyl cyanide-4-(trifluoromethoxy)-phenylhydrazone; GLUT – glucose transporter; HG – high glucose medium (25 mM); IMM – inner mitochondrial membrane; lncRNA – long non-coding RNA; NG – normal glucose medium (5.5 mM); NRF – nuclear respiratory factor; Omy – oligomycin; PGC-1α – peroxisome proliferator-activated receptor (PPAR) gamma coactivator 1-α; PI3K – phosphatidylinositol 3-kinase; Q – quercetin; Q3S – quercetin 3′-O-sulfate; Q3G – quercetin 3-O-β-D-glucuronide; RGMB – repulsive guidance molecule family member b; AS1 – anti-sense 1; Rot – rotenone; ROS – reactive oxygen species; ROX – residual oxygen consumption; SIRT – sirtuin; TBP – TATA-box binding protein; TFAM – mitochondrial transcription factor A; TR-FRET – time-resolved fluorescence energy transfer.

Graphical Abstract:

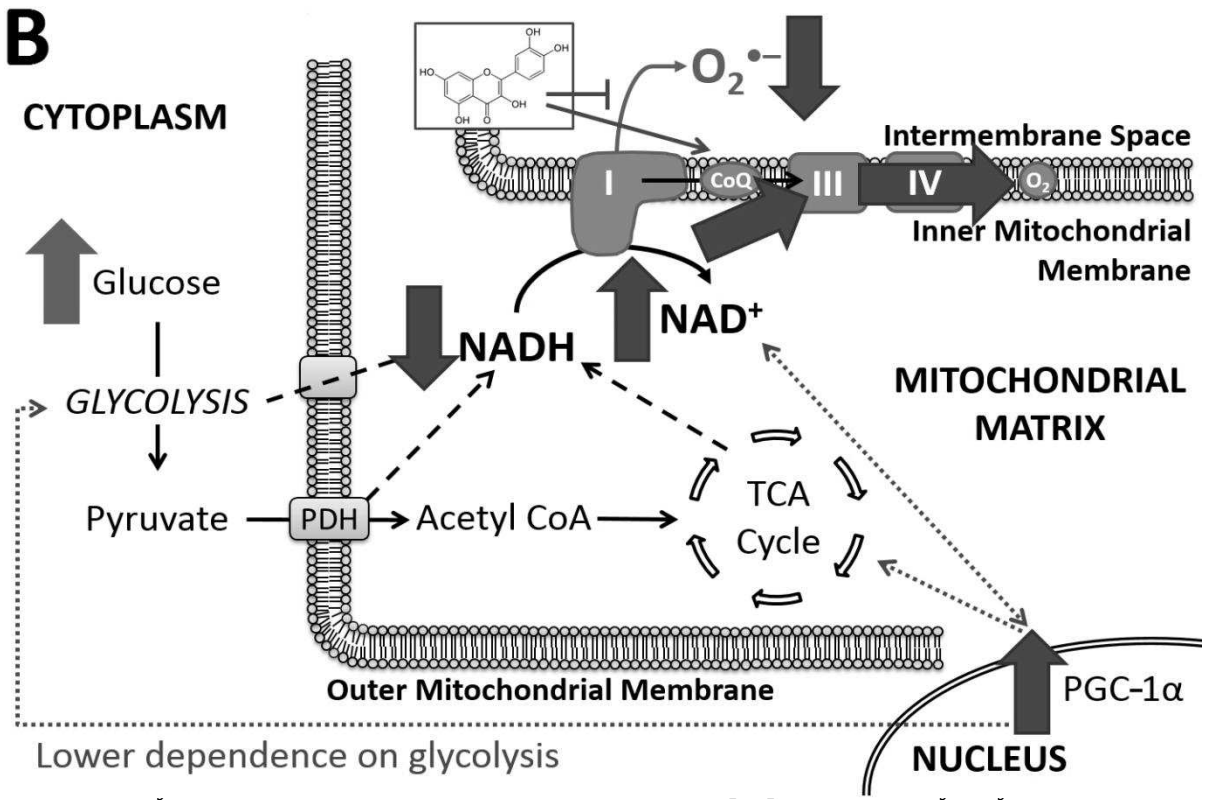

least in part as a result of the high glucose stress.

Quercetin is a well-studied flavonoid that transiently accumulates in mitochondria [16] following rapid passive cellular uptake or local de-conjugation of quercetin metabolites, especially at sites of inflammation [17-19]. Quercetin has been shown to exert an effect on mitochondrial function both directly and indirectly through signalling pathways associated with biogenesis, metabolic flux, respiration, mitochondrial membrane potential and apoptosis [16, 20, 21]. Studies in rat pancreatic cells suggest quercetin can improve mitochondrial bioenergetics by increasing respiration coupling efficiency [22] while in primary cortical neuronal cells quercetin enhanced respiratory capacity and cell survival [23]. Quercetin has also been shown to stimulate mitochondrial metabolic signalling pathways [23], and to increase PGC-1α, NRF-1 and TFAM mRNA both in HepG2 cells and mouse primary hepatocytes [24, 25].

At the same time quercetin and other flavonoids are also known to influence glucose in the intestine through modulation of carbohydrate digestion and absorption [26-28] and thus affect hepatic glucose, and expression of glycolytic genes in the liver [29]. In streptozotocin-induced diabetic rats, quercetin dose-dependently decreased blood glucose, cholesterol and triglycerides [30] alongside hepatic oxidative stress markers [31], while it increased hepatic glucokinase activity [30]. Such bioactivities have attracted research in the potential application of quercetin in the prevention and management of type 2 diabetes [32, 33], but data on its mechanism of action in high glucose stress environments is lacking.

The majority of previous in vitro studies examining the effects of quercetin on mitochondria have often employed acute treatments directly to isolated organelles [34-36], and overlooked longer-term effects in intact cells. In isolated rat brain mitochondria, quercetin lowered hydrogen peroxide production and inhibited complex I, while the latter was reversed by addition of coenzyme Q_{10} (CoQ) [34]. In comparison, in isolated mitochondria from rat duodenum quercetin protected complex I from inhibition by non-steroidal anti-inflammatory drugs, suggesting a CoQ-like function [35]. To enhance understanding of the role of quercetin on maintaining mitochondrial function, we evaluated its dose-dependent effects, following chronic application of up to 24 h, on mitochondrial respiration in an immortalized human hepatic cell model stressed by chronic high glucose.

Several studies have linked cancer phenotype progression, generally relying on fast glucose turnover and glycolysis, with expression levels of repulsive guidance molecules (RGM) [37-39]. The biological function of RGMs, a recently discovered family of glycosylphosphatidylinositol-linked cell-membrane-associated proteins, remains largely elusive but recent work has unveiled a discrete tissue-specific pattern of gene and protein expression for each member (a, b, c) [37]. RGMb is specifically thought to regulate respiratory immunity, while it's long non-coding RNA (lncRNA) RGMB-AS1 is lowly expressed in hepatocellular carcinoma tissues and cell lines [40, 41] and, as such, gain-of-function studies showed that up-regulation of lncRNA RGMB-AS1 suppressed proliferation, migration and invasion of hepatocellular carcinoma cells such as HepG2 and promoted cell apoptosis [40]. The effects of quercetin on RGMb and RGMB-AS1 are yet to be determined. We

demonstrate a link between oxidative signalling pathways and changes in mitochondrial respiration and metabolic phenotype in the glycolytic environment of HepG2 cells following chronic quercetin treatment, with an associated effect on RGMB(-AS1).

Materials and Methods

Chemical compounds and reagents

All cell culture medium components, quercetin 3-O-β-D-glucuronide and other reagents were from Sigma-Aldrich (Gillingham, UK) unless otherwise stated. Quercetin was from Extrasynthese (Genay, France) and quercetin 3′-O-sulfate was synthesised in house [42]. TrypLE Express and Pierce Coomassie (Bradford) Protein Assay Kit (#23200) were from Thermo Fisher Scientific (Paisley, UK). Mouse anti-NDUFB8 (ab 110242) was from Abcam (Cambridge, UK) and NADH was from VWR (Lutterworth, UK). FAM-labelled Taqman primers for PPARGC-1α (PGC-1α, Hs01016719_m1), Repulsive guidance molecule b (RGMB, Hs00543559_m1), RGMB antisense RNA 1 (RGMB-AS1, Hs04273852_m1) and VIC-labelled primer for TATA-box binding protein (TBP) primer (Hs00427620_m1) were from Life Technologies (Thermo Fisher Scientific). Droplet digital PCR (ddPCR) Supermix for Probes (no dUTP) and all other materials used for ddPCR were from Bio-Rad (Watford, UK). High purity water (18.2 MΩ cm^{-1}) supplied by a MilliQ system (Merck Millipore UK, Watford, UK) was used throughout this work.

Cell culture

HepG2 cells purchased from the American Type Culture Collection (HB-8065, LGC Promochem, Teddington, UK) were maintained in Eagle's minimum essential medium (EMEM) containing 5.5 (normal) or 25 mM (high) glucose, supplemented with 10% (v/v) heat-inactivated fetal bovine serum (FBS), 100 U/ml penicillin, 100 mg/ml streptomycin, 2% (v/v) non-essential amino acids, and 1% (v/v) sodium pyruvate. Cells were seeded in 75 cm^2 flasks, 6-well or 24-well plates (Appleton Woods, UK) at 8 x 10^4 cells cm^{-2} and kept in a humidified atmosphere of 5% CO_2/95% air at 37°C. The EMEM medium was supplemented with additional glucose and filtered through a 0.2 μm PTFE filter (Corning, UK) for high glucose conditions.

Trypan Blue exclusion cell viability assay

HepG2 cells were seeded in 75 cm^2 flasks or 6-well plates and maintained in normal or high glucose for 96 h. Medium was changed at 48 h after seeding and at 72 h cells were treated with 10 or 20 μM quercetin (or 0.1% DMSO controls) in full medium without FBS. After the 24 h treatments cells were lifted with 0.25% trypsin-EDTA or TrypLE Express, resuspended in 1 ml medium and an

aliquot mixed 1:1 (v/v) with 0.4% Trypan Blue-PBS. Resuspended cells were counted and assessed for Trypan Blue exclusion using a TC10 automated cell counter (Bio-Rad Laboratories, Hercules, CA, USA). Viable cells excluding Trypan Blue were expressed as a percentage of total cells counted.

Isolation of submitochondrial particles

HepG2 cells were seeded in 75 cm^2 flasks and grown in normal or high glucose for 96 h. Cells were treated with 2.5, 5, 10 or 20 µM quercetin (or 0.1% DMSO controls) for the final 24 h, scraped into 1 ml PBS supplemented with 1% (v/v) protease inhibitor cocktail (P8340, Sigma-Aldrich, UK), centrifuged at 210x g (4^oC, 5 min) and snap-frozen in ethanol over dry ice. Cell pellets were stored at -80^oC until mitochondrial isolation. Submitochondrial particles were prepared from thawed cell pellets following three freeze-thaw cycles [43-45], homogenisation with a Dounce homogenizer and differential centrifugation using the Mitochondria Isolation Kit for Cultured Cells (ab 110171, Abcam, UK) following the manufacturer's protocol guidelines but with an extra centrifugation step (1000x g, 4^oC, 5 min) at the end, for a purer preparation. Mitochondrial pellets were resuspended in 250 mM sucrose, 10 mM HEPES, 50 mM Tris buffer (pH 7.4) supplemented with 1% (v/v) protease inhibitor cocktail.

Submitochondrial fraction purity assessment

Aliquots of the initial cell lysate and the isolated submitochondrial particles of HepG2 cells were analysed for NDUFB8 (a subunit of complex I) levels by ProteinSimple Wes automated western blotting (ProteinSimple, Bio-Techne, CA, USA) according to the manufacturer's guidelines. Samples were denatured at 37^oC for 20 min and applied at 4.8 mg protein /ml with primary mouse anti-NDUFB8 at 1/50 dilution and chemiluminescence detected in the multi-image analysis mode. Data are presented as chemiluminescence peaks and in the traditional Western gel-like image view (Compass Software, Bio-Techne).

Complex I activity assay

Submitochondrial particles from HepG2 cells grown in normal or high glucose for 96 h and treated with varying concentrations of quercetin for the final 24 h were isolated as described above and assayed for complex I specific activity spectrophotometrically in 96-well plates on a PheraSTAR FS microplate reader (BMG LabTech, Germany) at 37^oC. Submitochondrial particles (10 µg) were mixed with 150 µM NADH and 50 µM coenzyme Q_1 (analog of coenzyme Q_{10}) and the decrease in absorbance at 340 nm was followed for 60 min, as previously described [44-48] following

optimisation for sample mass and NADH/CoQ1 concentrations. Specific activity was calculated by converting rate of absorbance change into rate of NADH decrease per mg of total protein [43] and expressed as % of normal glucose (0.1% DMSO control).

DCFH-DA assay

HepG2 cells were grown in 6-well plates for 96 h in normal or high glucose and treated for the final 2, 12 or 24 h with 2.5, 5, 10 or 20 µM quercetin (or 0.1% DMSO controls). The DCFH-DA assay was used to assess oxidative stress as described before [49], but with the following modifications. Cells were washed with PBS, incubated with 10 µM DCFH-DA in PBS (37^{o}C, 20 min in darkness), washed again and fluorescence of DCF was measured on the PheraStar FS microplate reader (BMG LabTech, Germany; Ex/Em = 485/530 nm). Cells were scraped in CellLytic M supplemented with 1% (v/v) protease inhibitor cocktail and total protein was measured with the Bradford assay [50, 51]. DCF fluorescence, in relative fluorescence units, was corrected for protein and expressed as relative DCF fluorescence % in the normal/high glucose controls accordingly.

Citrate synthase activity assay

Cells were grown in 75 cm^2 flasks in normal or high glucose for 96 h, with 10 or 20 µM quercetin (or 0.1% DMSO controls) for the final 24 h. Cell pellets, prepared as above for mitochondria isolation, were lysed and assayed for citrate synthase activity, a marker for total mitochondrial content [52], using the Citrate Synthase Assay Kit (CS0720, Sigma-Aldrich) and following the manufacturer's instructions. Briefly, formation of the 5-thio-2-nitrobenzoic acid colorimetric reaction product was followed on the PheraStar FS microplate reader at 412 nm (30^{o}C, 5 min) and again after addition of oxaloacetic acid. Citrate synthase activity was calculated by correcting for the initial reaction rate, a baseline of endogenous thiol/deacetylase levels, and for total protein prior to the assay.

High-resolution respirometry

HepG2 cells, treated as for the citrate synthase assay, were washed in PBS, lifted from 75 cm^2 flasks using TrypLE Express and resuspended in serum-free medium at 1.5 x 10^6 cells/ml. Oxygen concentration and flux were continuously measured following addition of 2 ml of the cell suspensions to each chamber of the Oxygraph-2k (O2k) (OROBOROS Instruments, Innsbruck, Austria), maintained at 37^{o}C. A phosphorylation control protocol was followed [53, 54]. Routine respiration was initially recorded, followed by Leak measurement after addition of 250 nM oligomycin; titration with FCCP (carbonyl cyanide-4-(trifluoromethoxy)-phenylhydrazone) (5 µM, 3-5 µl) for ETS

capacity; and addition of 1.25 µM rotenone and 2.5 µM antimycin A for assessment of residual oxygen consumption (ROX). Additional experiments were conducted whereby quercetin (10-100 µM) was titrated directly into the respirometer chamber containing a HepG2 cell suspension, followed by FCCP positive control, to assess if quercetin was acting as a direct ETS uncoupler. As a control for the effect of quercetin reacting directly with oxygen, quercetin (10-200 µM) was also titrated into cell-free medium.

Cellular NAD^+/NADH assay

Cells were grown in 24-well plates and treated as described above for the DCFH-DA assay. Cells were washed in PBS, lysed and collected, and NAD^+/NADH was measured using a Fluorometric Assay Kit (ab 176723, Abcam, UK), in which enzymes specifically recognise NAD^+ or NADH in an enzyme cycling reaction. According to manufacturer's instructions, lysates were transferred to a black, clear-bottomed 96-well plate (Greiner Bio-One, Stonehouse, UK) and, after incubation for 60 min at RT, fluorescence signals were collected on the PheraSTAR FS (Ex/Em = 540/590 nm).

RNA isolation and cDNA synthesis

Cells were grown in normal or high glucose in 6-well dishes for 60 h. At 60 h cells were transferred to medium ± FBS for 12 h (72 h) before treatment with 20 µM quercetin (or 0.1% DMSO controls) for up to a further 24 h. Samples were collected after 1, 3, 6, 12 and 24 h. Additional samples were collected at 60 h (-12 h) and 72 h (time 0) in order to assess whether the absence of FBS had an effect on mRNA expression. Total RNA was isolated using the Aurum Total RNA Mini Kit (#732-6820, Bio-Rad Laboratories, UK) and following the manufacturer's instructions. RNA content was determined spectrophotometrically at 260 nm on a NanoDrop (Thermo Fisher Scientific) and cDNA was synthesised from 1 µg RNA using a High Capacity RNA-to-cDNA kit (Applied Biosystems, Thermo Fisher Scientific), following the manufacturer's guidelines.

Droplet digital PCR analysis

The QX100 Droplet Digital PCR system (Bio-Rad Laboratories, USA) was used to quantify changes in gene expression of PGC-1α, RGMB, RGMB-AS1 and TBP (housekeeping gene) as previously described [55]. Primers of PGC-1α, RGMB, RGMB-AS1 were mixed with TBP Taqman primer in a 20 µl assay (1 µl of each) that contained 10 µl of ddPCR Supermix and 8 µl of cDNA diluted with MilliQ water. The mixtures were dispersed into oil droplets using the QX100 Droplet

generator and then transferred to a C1000 Touch thermal cycler (Bio-Rad Laboratories, USA). Droplet-containing mixtures were incubated for 10 min at 95°C, followed by 40 cycles of 0.5 min at 94°C and 1 min at 57.8°C, and finished with 10 min incubation at 98°C. Products were maintained at 12°C before analysis on a QX100 Droplet Reader. The QuantaSoft software (Košice, Slovakia) was used to analyse the data and determine concentrations of the target DNA in copies per µl from the fraction of positive reactions using Poisson distribution analysis. Data were collected independently for each target and TBP and are presented as fold-change of control treatment.

PPAR*α* coactivator recruitment assay

The potential of quercetin to bind to PPARα and affect coactivator (PGC1-α) recruitment was tested both in the agonist and antagonist mode with a LanthaScreen TR-FRET (time-resolved fluorescence energy transfer) assay (#PV4684, Invitrogen, Thermo Fisher Scientific, UK) according to supplier's guidelines. Briefly, PPARα ligand binding domain tagged with glutathione-S-transferase (GST) was added either to GW7647 (PPARα agonist positive control), GW9662 (antagonist positive control), quercetin, quercetin 3′-O-sulfate or quercetin 3-O-β-D-glucuronide, followed by the addition of pre-mixed fluorescein- PGC-1α coactivator peptide (in 50 mM HEPES, pH 7.5) and LanthaScreen terbium-labelled anti-GST antibody (in 137 mM NaCl, 2.7 mM KCl, 10 mM HEPES, pH 7.5). Following optimization by comparison of achieved Z´ values, calculated by using the "maximum agonist" or "maximum antagonist" and "no agonist" or "no antagonist" control data [56], incubation was set at 3 h for the agonist mode assays and at 2 h for the antagonist mode (both at room temperature). The TR-FRET ratio was calculated by dividing the Em at 520 nm by the Em at 490 nm measured on a PheraStar FS microplate reader with a LanthaScreen filter module. The EC_{50} and IC_{50} values were calculated by GraphPad Prism 6 after fitting the data on an equation for a sigmoidal dose response.

Statistical analysis

Data are expressed as means ± standard error of the mean. The significance of differences between groups of treatments was analysed by one-way ANOVA and post hoc Tukey's, Dunnett's or two-tailed t-tests as indicated, with variance checks using Levene's test, and with Bonferroni correction when multiple treatments were compared with an independent samples Student t-test, using SPSS 24.

Results

Quercetin restores complex I activity compromised by chronic high glucose stress

The mitochondria isolation procedure yielded a highly purified fraction as confirmed by NDUFB8 (a subunit of complex I) expression (Fig. 1A). Complex I activity, as assessed by NADH oxidation in mitochondria isolated from HepG2 cells (Fig. 1B), decreased by 11% ($p < 0.001$) following high glucose for 24 h and by 19% ($p < 0.001$) after 96 h when compared to control cells. Both hydrogen peroxide and serum absence also decreased complex I activity, while, as expected, it was higher in cells grown in galactose-containing medium (Fig. 1C-D). In normal glucose, quercetin treatment (2.5-20 µM) caused a small decrease in complex I activity, comparable in all tested concentrations. However, in high glucose, quercetin up to 10 µM dose-dependently attenuated the high glucose-induced damage; a 94% recovery was found with 10 µM ($p < 0.001$) while at 20 µM the effect was less pronounced (Fig. 1E).

Quercetin lowers concentration of several ROS species in normal and high glucose

High glucose treatment for 96 h increased DCF fluorescence by 10% ($p < 0.01$) (Fig. 2A), indicating higher levels of some ROS species and an environment with increased oxidative stress. This was attenuated in both normal and high glucose conditions dose-dependently by quercetin (2.5-20 µM) at all the time points tested, up to 24 h (Fig. 2B-D). The effect of quercetin on DCF fluorescence was most evident at earlier time points, with a maximum lowering effect of 53% in normal ($p < 0.001$) and 57% in high glucose ($P < 0.001$) after treatment with 20 µM quercetin for 2 h (Fig. 2B). This highly significant decrease of ~45% in the DCF fluoresce signal in both normal and high glucose conditions is indicative that some ROS species were decreased, and this decrease was not significantly different between normal and high glucose with any dose of quercetin at 2 h (Fig. 2B). Quercetin effects were less evident at later time points, particularly in the high glucose (Fig. 2C-D). Although we observed changes at 2.5 µM and above, in subsequent experiments we chose to test 10 and 20 µM quercetin to clarify the mechanism of protection against high glucose.

Quercetin decreases mitochondrial content while increasing cell viability

Growing cells in normal or high glucose did not affect citrate synthase activity, a mitochondrial matrix marker, whereas quercetin significantly lowered citrate synthase activity after 24 h in normal glucose at 10 and 20 µM by 5 and 7% ($p < 0.05$) respectively. In high glucose an effect was observed only with the 20 µM treatment (5%, $p < 0.05$) (Fig. 3A). Cell viability, assessed by Trypan Blue

exclusion, was also not affected by glucose but dose-dependently increased by quercetin, by up to 5% in high glucose ($p < 0.001$) (Fig. 3B).

Quercetin lowers high glucose-induced proton leak and increases oxidative respiration

Inner mitochondrial membrane (IMM) proton leak, was 21% ($p < 0.05$) higher in high glucose-treated cells, which was reflected in lower coupling efficiency ($p < 0.01$), but without significant changes in basal Routine respiration, non-coupled ETS capacity, or non-ETS residual oxygen consumption (ROX). Despite less efficient coupling, mitochondrial ATP production was unaffected (Fig. 4B). Respiration in normal glucose was unchanged by quercetin, but Leak was hormetically suppressed ($p < 0.01$) and coupling efficiency was higher with 10 µM accordingly ($p < 0.05$) (Fig. 4C). Quercetin treatment dose-dependently reversed the high glucose-induced proton Leak ($p < 0.01$) (Fig. 4D) while 10 µM quercetin also increased oxidative respiration; both the basal cellular and the oligomycin-sensitive 'Net' mitochondrial respiration (calculated from (Routine-Leak)/ETS) ($p < 0.01$). Moreover, mitochondrial ATP production was enhanced ($p < 0.01$) and coupling efficiency recovered ($p < 0.001$) (Fig. 4D). A similar effect was not evident with 20 µM quercetin treatment (Fig. 4D). In general, following quercetin treatment, ETS capacity was either unchanged (normal glucose, 10 µM quercetin) or mildly lower (both in normal and high glucose), and ROX was dose-dependently decreased in both normal and high glucose (Fig. 4C-D).

Quercetin does not uncouple mitochondrial respiration

When added directly to cell-free medium in the respirometer, quercetin dose-dependently reacted with oxygen (Fig. 5A). When added to HepG2 cells in suspension and equilibrated in the respirometer chamber, the increase in oxygen consumption was no longer evident, indicating quercetin did not react with oxygen in the medium in the presence of the cells, but was rather rapidly taken up. In the cellular environment quercetin did not act as a direct ETS uncoupler, unlike FCCP (Fig. 5B).

Quercetin reversed the decreased NAD^+/NADH in high glucose within 2 h

High glucose increased cellular NADH ($p < 0.001$) (Fig. 6A), but this was blunted at later time-points. Quercetin dose-dependently increased NAD^+/NADH in high glucose after 2 h ($p < 0.01$), but not in normal glucose (Fig. 6A). NAD^+/NADH was elevated after 12 h with 10 µM quercetin in both normal and high glucose ($p < 0.001$) (Fig. 6B) and this effect was maintained in normal glucose

up to 24 h ($p < 0.001$) (Fig. 6C). In high glucose, an effect was evident with 20 µM quercetin at 24 h ($p < 0.05$).

Quercetin increased PGC-1*α*, RGMB and RGMB-AS1 mRNA

Absence of serum increased PGC-1α mRNA expression under both normal and high glucose conditions (Fig. 7A, 7C) while RGMB and RGMB-AS1 mRNA levels were not affected by either (Fig. 9, 10-panels A, C). Following 12 h in serum-free medium (time 0) PGC-1α increased by 1.7-fold ($p < 0.001$) and remained stable for 12 h in normal glucose before returning to basal levels by 24 h (Fig. 7A). In the presence of high glucose a further increase was evident at 6 h (2-fold), while at 24 h mRNA levels were significantly lower than in control cells (Fig. 7C). Treatment with 20 µM quercetin increased PGC-1α gene expression within 1 h in normal glucose ($p < 0.001$) and within 6 h in high glucose ($p < 0.001$). A maximal approximately 2-fold effect was reached at 6 h in both normal and high glucose (Fig. 7E, 7G). Quercetin increased RGMB mRNA ~5-fold after 3 h ($p < 0.001$) (Fig. 9E, 9G) and RGMB-AS1 ~3.5-fold after 6 h ($p < 0.001$) (Fig. 10E, 10G), similarly in normal and high glucose. Increased mRNA levels of RGMB and RGMB-AS1 were maintained until at least for 12 h. As the droplet digital PCR technique determines the absolute number of mRNA molecules in the reaction, employing a stably expressed reference gene is not essential but TBP was used to account for variations in the sample preparation and to provide comparison between different conditions. TBP was mildly affected by the absence of serum and the high glucose conditions and therefore was reported separately (Fig. 7, 9, 10- B, D, F, H) to avoid bias of the results. TBP signals were similar when multiplexing with the different primers (PGC-1α, RGMB, RGMB-AS1) in all experiments.

Quercetin *does not affect PPARα coactivator recruitment* of PGC1-*α*

A TR-FRET assay was set up to test if quercetin could directly affect binding of PGC-1α to PPARα. The assay was able to detect binding interactions with high sensitivity and small variability; a Z′ of 0.851 and an EC_{50} of 1.057 nM was measured for GW7647 (Fig. 8A), and a Z′ of 0.689 and an IC_{50} of 443.6 nM for GW9662 (Fig. 8B), a known agonist and antagonist of PPARα respectively. Quercetin was found to exert only minimal effects in the agonist mode at ≥ 10 µM ($p < 0.01$) (Fig. 8C), while it had no effect as an antagonist (Fig. 8D). An EC_{50} was not calculated for quercetin because for the concentrations tested a plateau was not reached (Fig. 8C). Quercetin conjugates, quercetin 3′-O-sulfate and quercetin 3-O-β-D-glucuronide, were weaker agonists than quercetin aglycone; an increase in fluorescence emission was measured only at ≥ 100 µM ($p < 0.01$) (Fig. 8C).

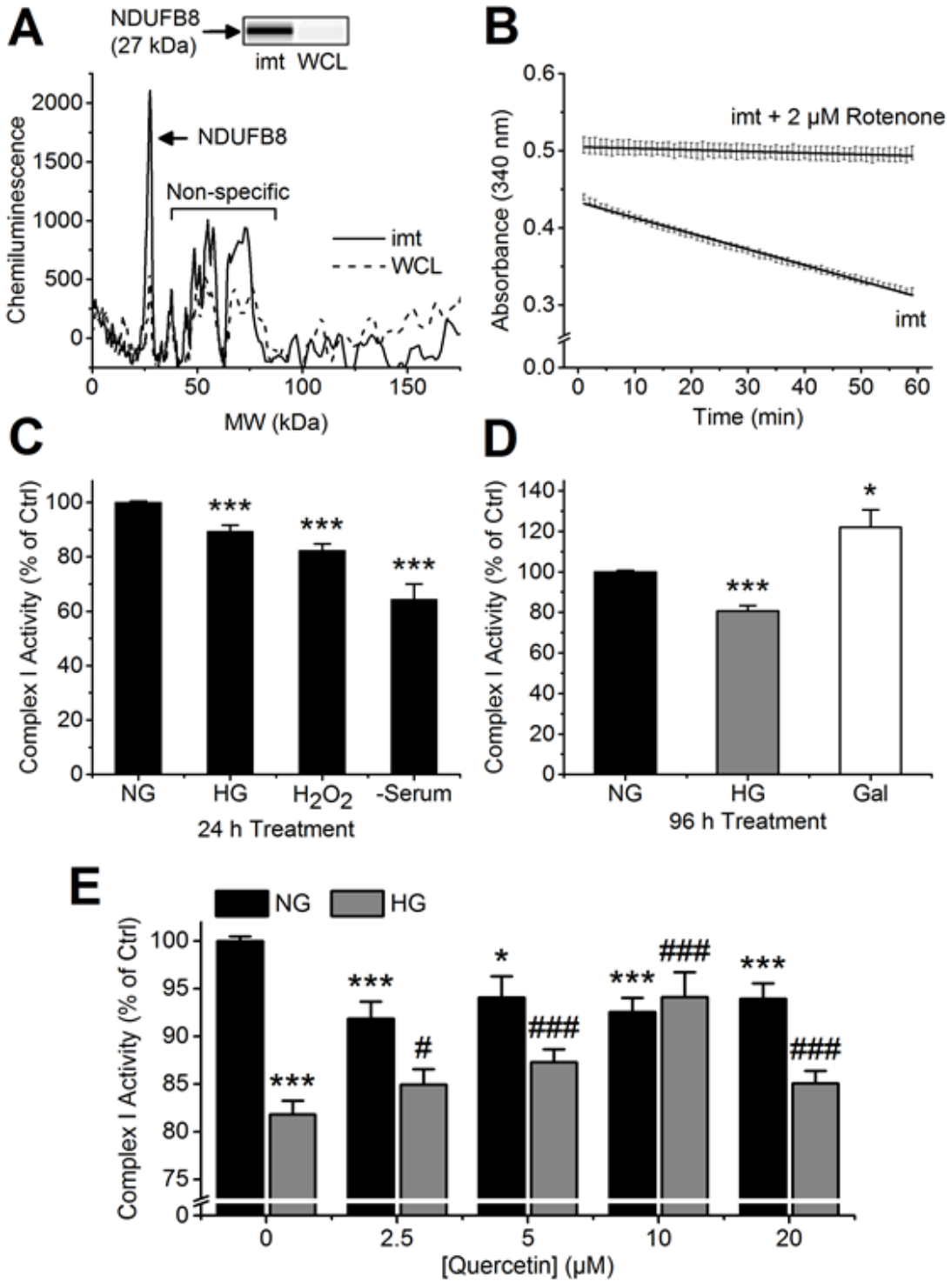

Fig. 1. Quercetin dose-dependently recovered complex I activity decreased by high glucose in HepG2 cells. (A) Purity of isolated mitochondrial fraction (imt). Protein expression of complex I subunit NDUFB8 increased when compared to the whole cell lysate (WCL), assessed by ProteinSimple

automated Western, with traditional Western blot and pherogram views. (B) Complex I activity in 10 µg imt assessed with NADH (150 µM) in the presence of coenzyme Q_1 (50 µM), and corrected for non-mitochondrial oxidation by rotenone-inhibited (2 µM) control. Lines of best fit for mean activity ± SEM. (C) Complex I activity in cells grown in normal glucose (NG) medium supplemented with 10% serum for 72 h and then treated for 24 h with high glucose (HG), 0.5 mM hydrogen peroxide (H_2O_2) or serum-free medium. Complex I activity was normalised to the NG control (13.7 ± 0.8 nmol/min/mg) and data are expressed as mean percentages ± SEM (N/n = 3/9). ***$p < 0.001$ vs NG control. (D) Complex I activity in cells grown for 96 h in NG, HG or 10 mM galactose (Gal); data are expressed as mean percentages of NG ± SEM (NG = 8.9 ± 0.9 nmol min^{-1} mg^{-1}) (N/n = 5/15). *$p < 0.05$, *** $p < 0.001$ vs NG control. (E) Complex I activity in cells grown for 96 h in NG or HG and treated for the final 24 h (in the absence of serum) with various concentrations of quercetin (or DMSO controls). Data are mean percentages of the NG control ± SEM (NG = 8.6 ± 0.3 nmol/min/mg) (N/n = 6/18). *$p < 0.05$, ***$p < 0.001$ vs NG control; $^{\#}p < 0.05$, $^{\#\#\#} < 0.001$ vs HG control.

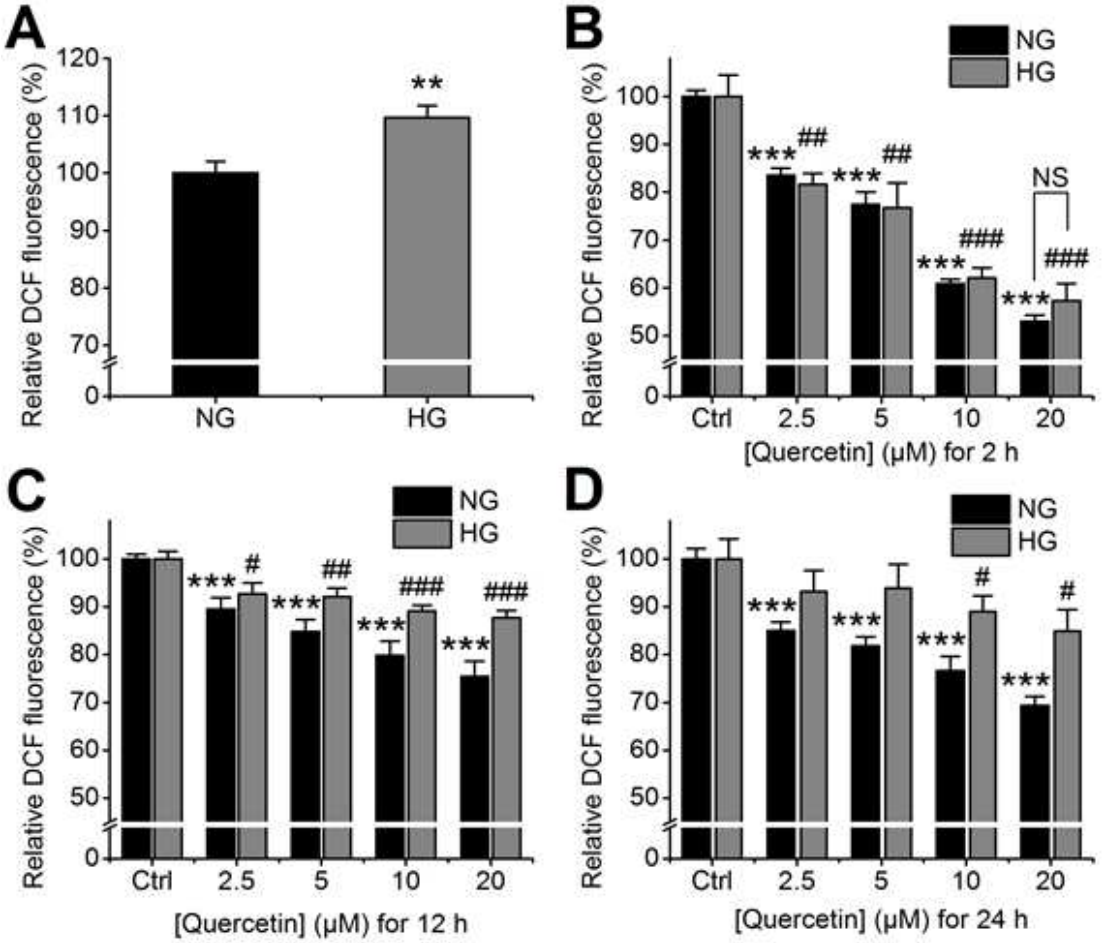

Fig. 2. Quercetin decreased the relative DCF fluorescence in normal and high glucose HepG2 cells. (A) Cells were grown for 96 h in normal (NG) or high (HG) glucose and then incubated with 10 µM DCFH-DA (20 min), relative fluorescence of DCF was measured and corrected for total protein. (B-D) Cells grown in NG or HG for 96 h were treated with quercetin (or DMSO control), in the absence of serum, for the final 2 h (B), 12 h (C) or 24 h (D) and DCF measured in the same way. All data are mean values expressed as (%) of the NG or HG controls accordingly ± SEM (N/n = 4/12). **$p < 0.01$, ***$p < 0.001$ vs NG controls; $^{\#}p < 0.05$, $^{\#\#}p < 0.01$, $^{\#\#\#}p < 0.001$ vs HG controls; NS = not significant.

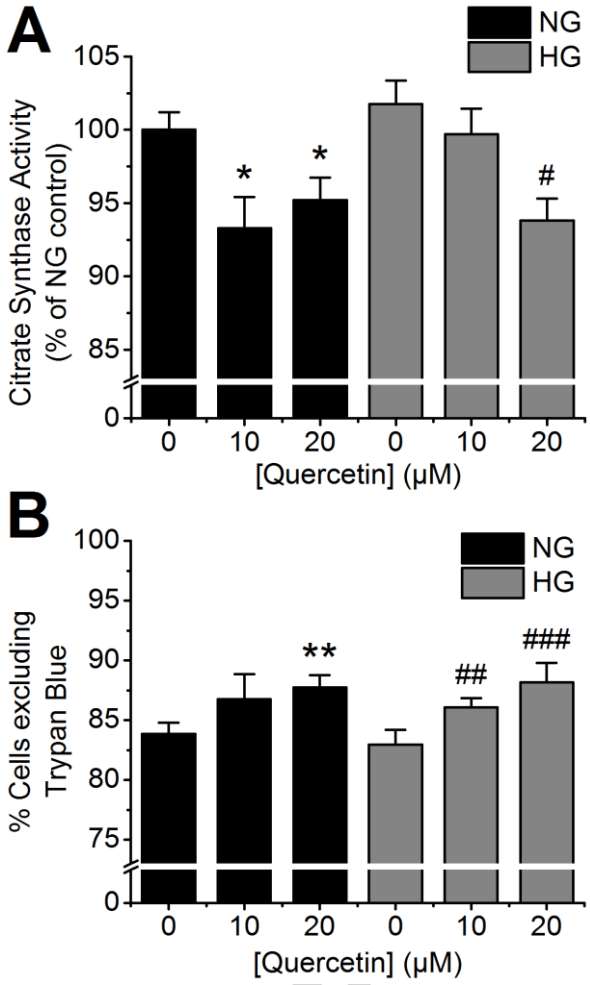

Fig. 3. Quercetin decreased mitochondrial citrate synthase and increased viability in HepG2 cells. (A) Mitochondrial citrate synthase activity in cells grown for 96 h in normal (NG) or high (HG) glucose and treated for the final 24 h, in the absence of serum, with 10 or 20 µM quercetin (or DMSO control). All data are mean values expressed as (%) of the NG control ± SEM (NG = 43.8 ± 0.5 nmol min^{-1} mg^{-1}) (N = 6 for 10 µM; 9 for 20 µM; 15 for controls). *p < 0.05 vs NG control; $^{\#}$p < 0.05 vs HG control. (B) Cells were assessed for plasma membrane integrity using the Trypan Blue exclusion test. Data are mean values of cells that excluded Trypan Blue expressed as (%) of total cells ± SEM (N = 6 for 10 µM; 13 for 20 µM; 19 for controls). **p < 0.01 vs NG control; $^{\#\#}$p < 0.01 vs HG control; $^{\#\#\#}$p < 0.001 vs HG control.

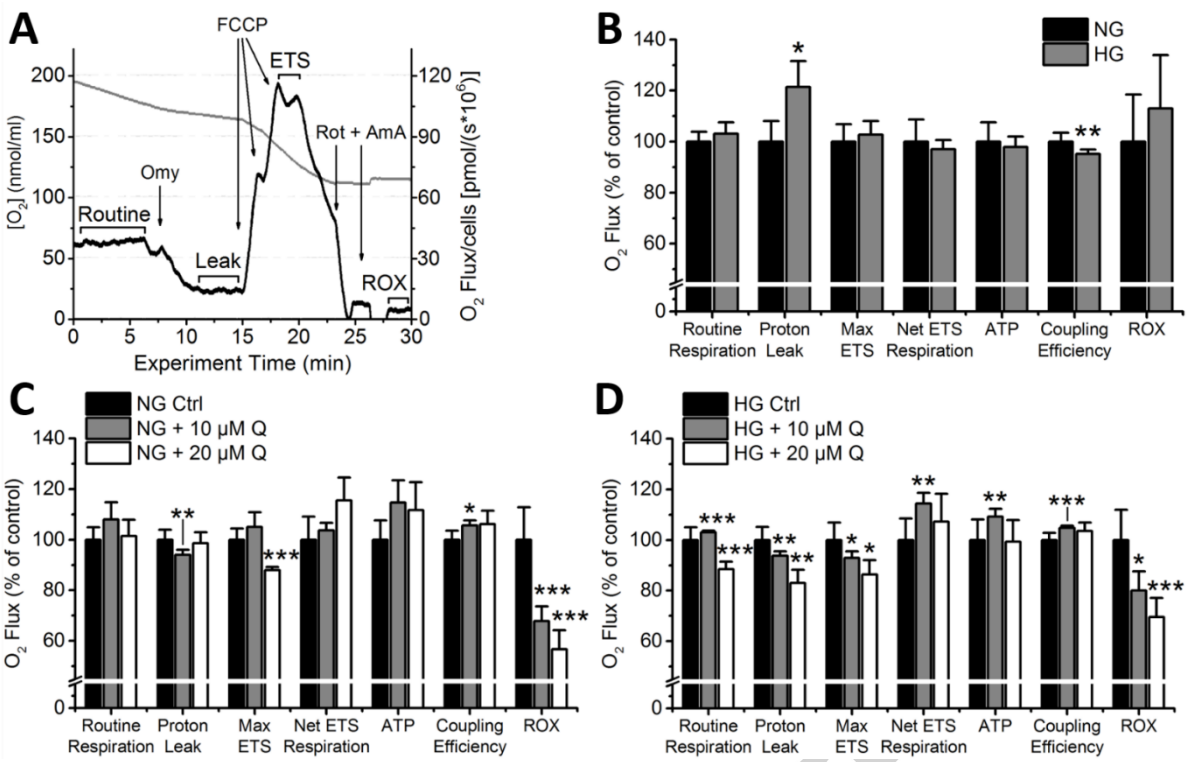

Fig. 4. Quercetin decreased high glucose-induced IMM proton leak and increased oxidative respiration. (A) Typical oxygen flux trace from an experiment using the OROBOROS O2k high-resolution respirometer (grey line – $[O_2]$; black line – O_2 flux). Intact HepG2 cells were added to the respirometer and, following equilibration, respiration states were measured in turn for Routine Respiration, Proton Leak (after addition of oligomycin (250 nM) (Omy)), maximal electron transfer system capacity (ETS) (uncoupled by FCCP (5 µM) titration), and non-ETS residual oxygen consumption (ROX) (addition of rotenone (1.25 µM) (Rot) and antimycin A (2.5 µM) (AmA)). Routine, Leak and ETS data were all ROX-corrected. (B) Respirometry data for cells grown in normal (NG) or high (HG) glucose for 96 h. Net ETS Respiration is the net routine flux control ratio, calculated as ((Routine-Leak)/ETS), and is the ratio of basal ETS respiration driving mitochondrial ATP production as a factor of the maximal ETS capacity. ATP is ATP production, calculated as oligomycin-sensitive respiration (Routine-Leak). Coupling efficiency is the ratio of ATP production/Routine Respiration. Data shown are mean values and expressed as (%) of the NG control ± SEM (N = 9). *p < 0.01 vs NG. (C-D) Cells grown in NG (C) or HG (D) for 96 h were treated with 10 or 20 µM quercetin (Q) (or DMSO controls), in the absence of serum, for the final 24 h. Data are mean values and expressed as (%) of the NG or HG control accordingly ± SEM (N = 5 for 10 µM; 9 for 20 µM; 14 for controls). *p < 0.05, **p < 0.01, ***p < 0.001 vs controls. See Supplementary Table 1 for control values.

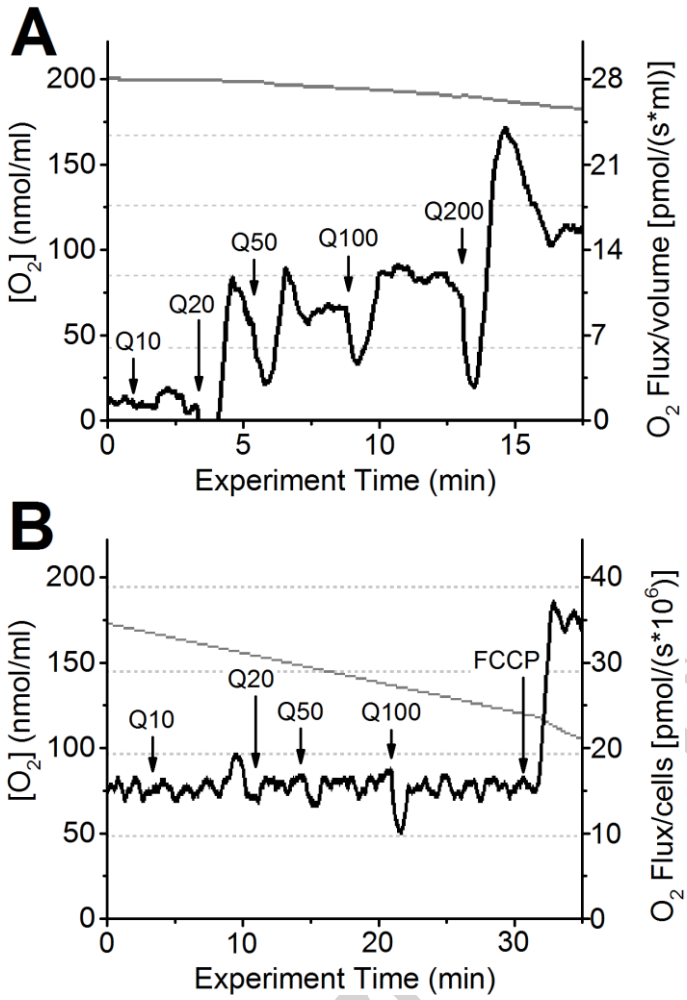

Fig. 5. Quercetin reacts with oxygen and is rapidly taken up by HepG2 cells without uncoupling ETS. (A) Oxygen 'flux' trace for cell-free medium when titrated with quercetin (10-200 µM final) in the OROBOROS O2k high-resolution respirometer. (B) Intact HepG2 cells were added to the respirometer and, following equilibration, quercetin (10-100 µM) was titrated in, followed by a single addition of FCCP (5 µM) as a positive control. Grey line – $[O_2]$; black line – O_2 flux; Q followed by number indicates cumulative quercetin concentration (µM).

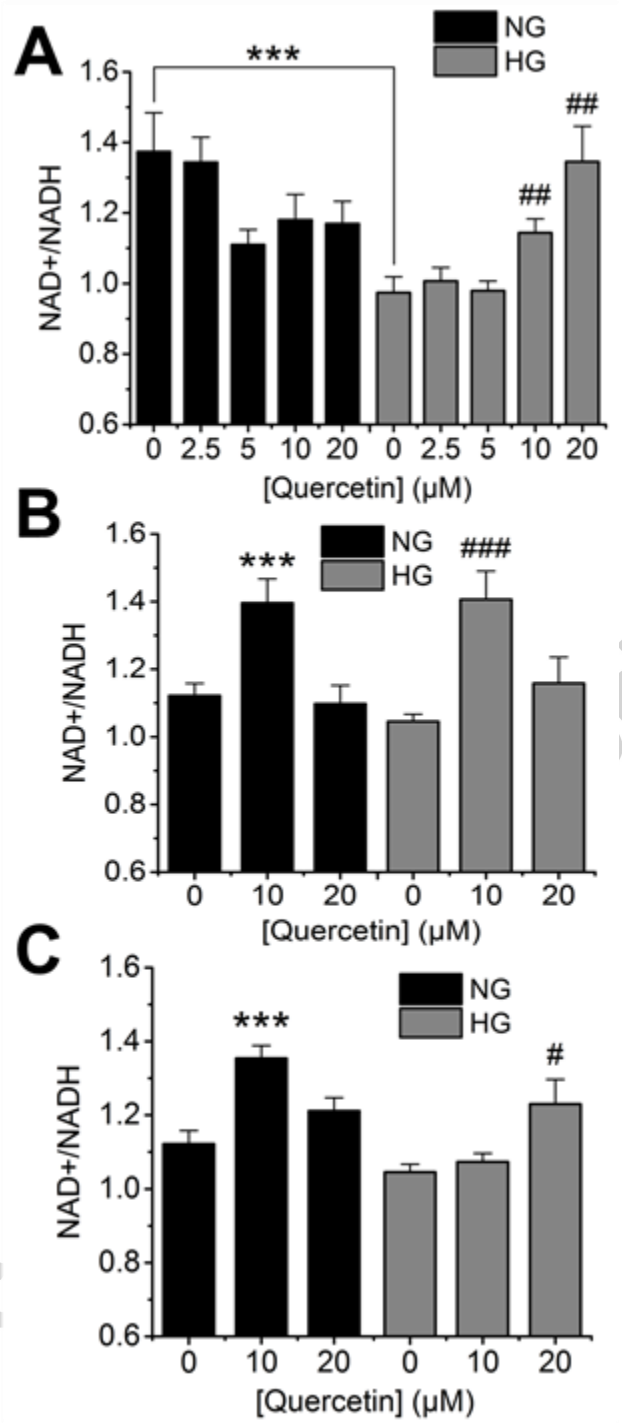

Fig. 6. Quercetin reversed the high glucose-decreased NAD^+/NADH ratio in HepG2 cells. (A) Cells grown in normal (NG) or high (HG) glucose for 96 h were treated with various concentrations of quercetin (or DMSO controls) for the final 2 h. (B-C) NG and HG cells were treated with 10 or 20 μM quercetin (or DMSO controls) for the final 12 h (B) or 24 h (C). All data are expressed as mean NAD^+/NADH ± SEM (N/n = 6/36). ***$p < 0.001$ vs NG control; $^{\#}p < 0.05$, $^{\#\#}p < 0.01$, $^{\#\#\#}p < 0.001$ vs HG control.

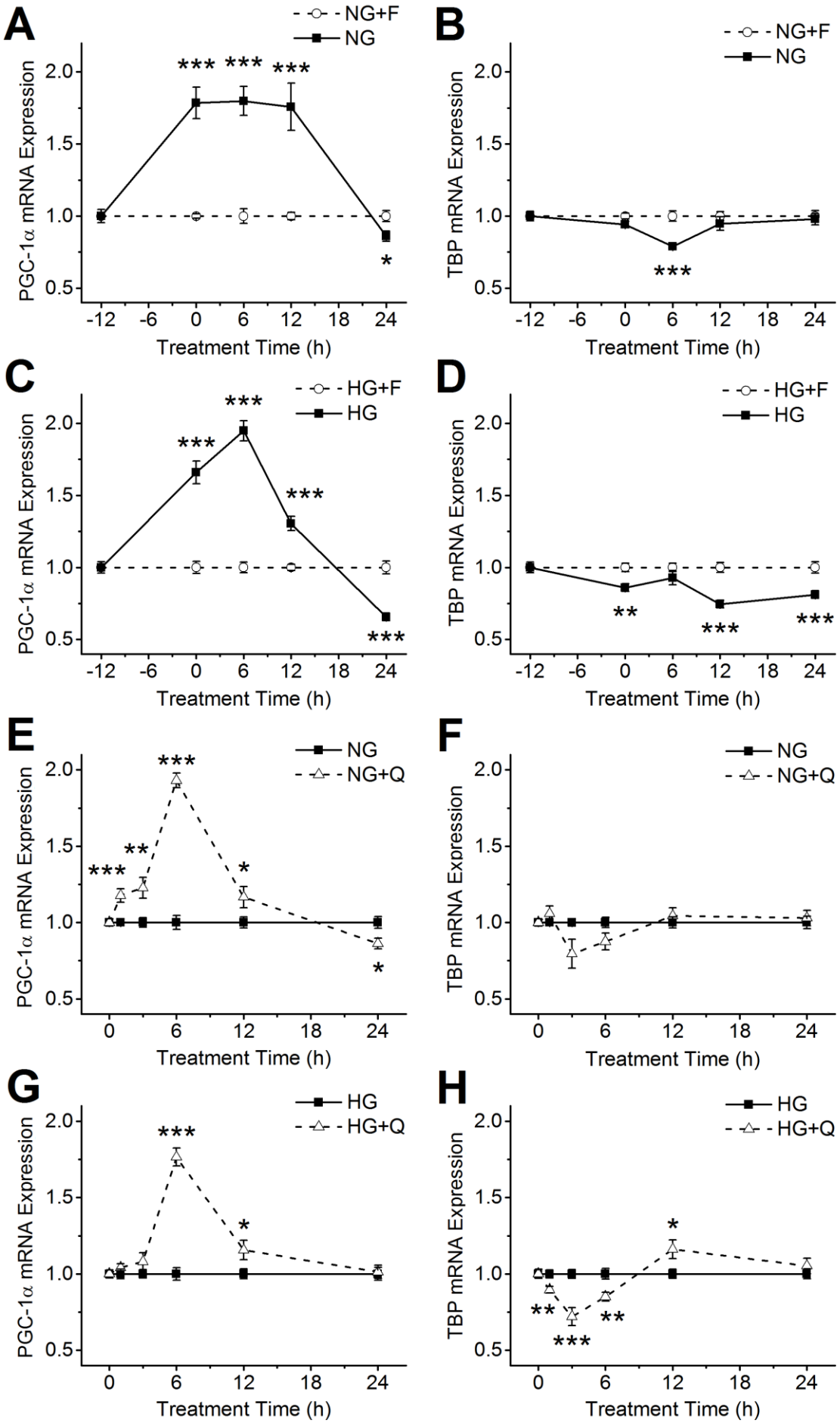
A
NG+F
NG
PGC-1α mRNA Expression
Treatment Time (h)
B
TBP mRNA Expression
C
HG+F
HG
D
E
NG+Q
F
G
HG+Q
H

Fig. 7. PGC-1α and TBP mRNA expression following 12h serum starvation in normal and high glucose-treated HepG2 cells (A-D). PGC-1α and TBP mRNA levels following quercetin treatment (E-H).Cells were seeded in normal (NG) or high (HG) glucose media and after 60 h (T = -12 h) the medium was changed to medium ± FBS (F). Cells were treated at 72 h (T = 0 h) with ± FBS and lysates for RNA extraction were collected at 6, 12 and 24 h, with additional at -12 and 0 h. (E-H) Cells were grown in the same way and treated with serum-free medium from 60 h and with 20 μM quercetin (Q) at 72 h (T = 0 h) (or DMSO controls), and samples were collected at 1, 3, 6, 12 and 24 h. All data are mean values of fold-change in PGC-1α or TBP expression ± SEM (N/n = 6/18) vs respective controls. *$p < 0.05$, **$p < 0.01$, ***$p < 0.001$ vs respective control.

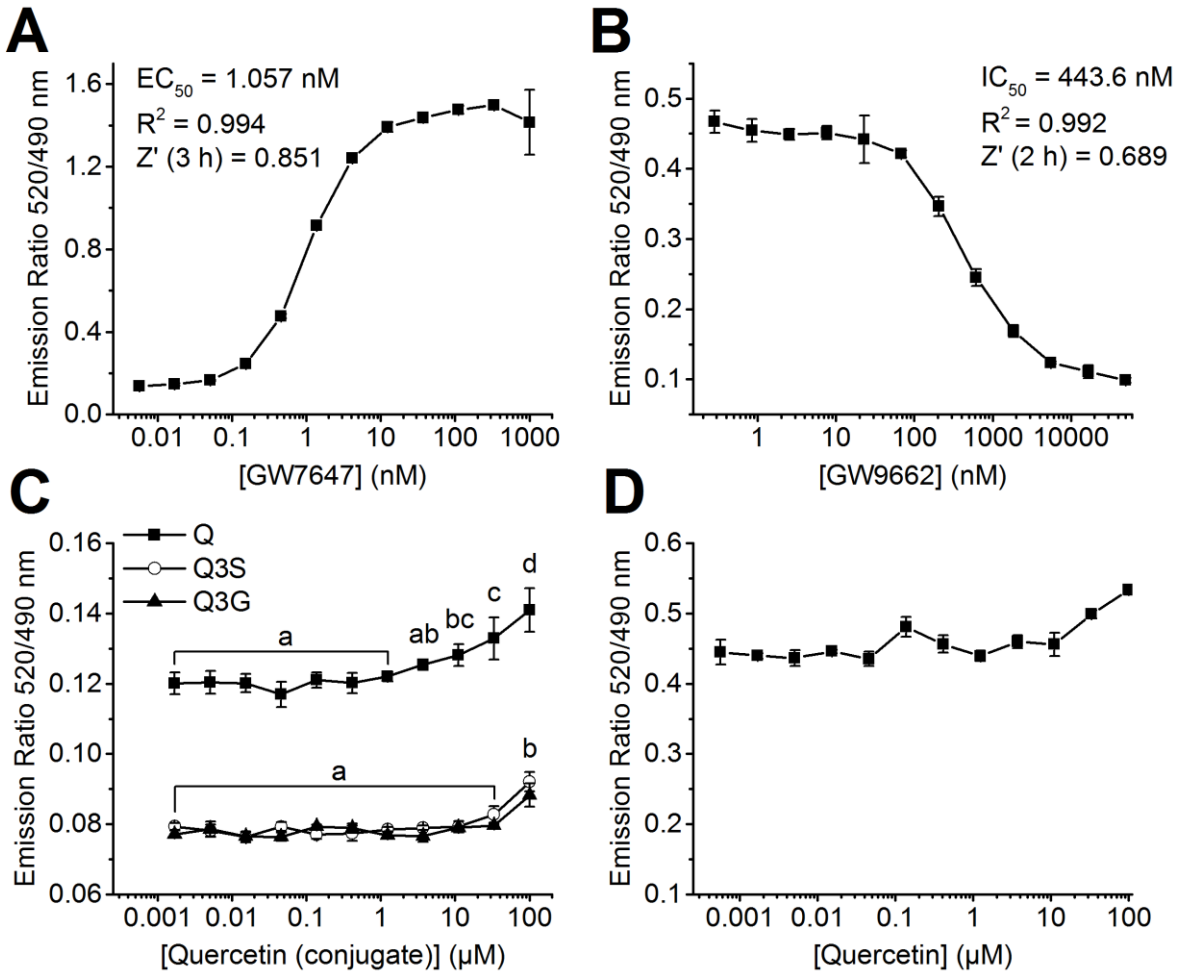

Fig. 8. Quercetin increased coactivator recruitment of PGC-1α to PPARα in vitro only at ≥ 10 µM. (A) An EC_{50} of 1.057 nM was measured for GW7647. (B) An IC_{50} of 443.6 nM was measured for GW9662. (C) Quercetin (Q), quercetin 3′-O-sulfate (Q3S) and quercetin 3-O-β-D-glucuronide (Q3G) were tested in the agonist mode at 0.6-100 µM (A). Letters indicate significant differences between tested concentrations compared by one-way ANOVA and Bonferroni correction ($p < 0.01$). (D) Quercetin had no effect as an antagonist at the tested concentrations (0.6-100 µM). All data are mean (N/n = 3/18) and error bars represent SEM.

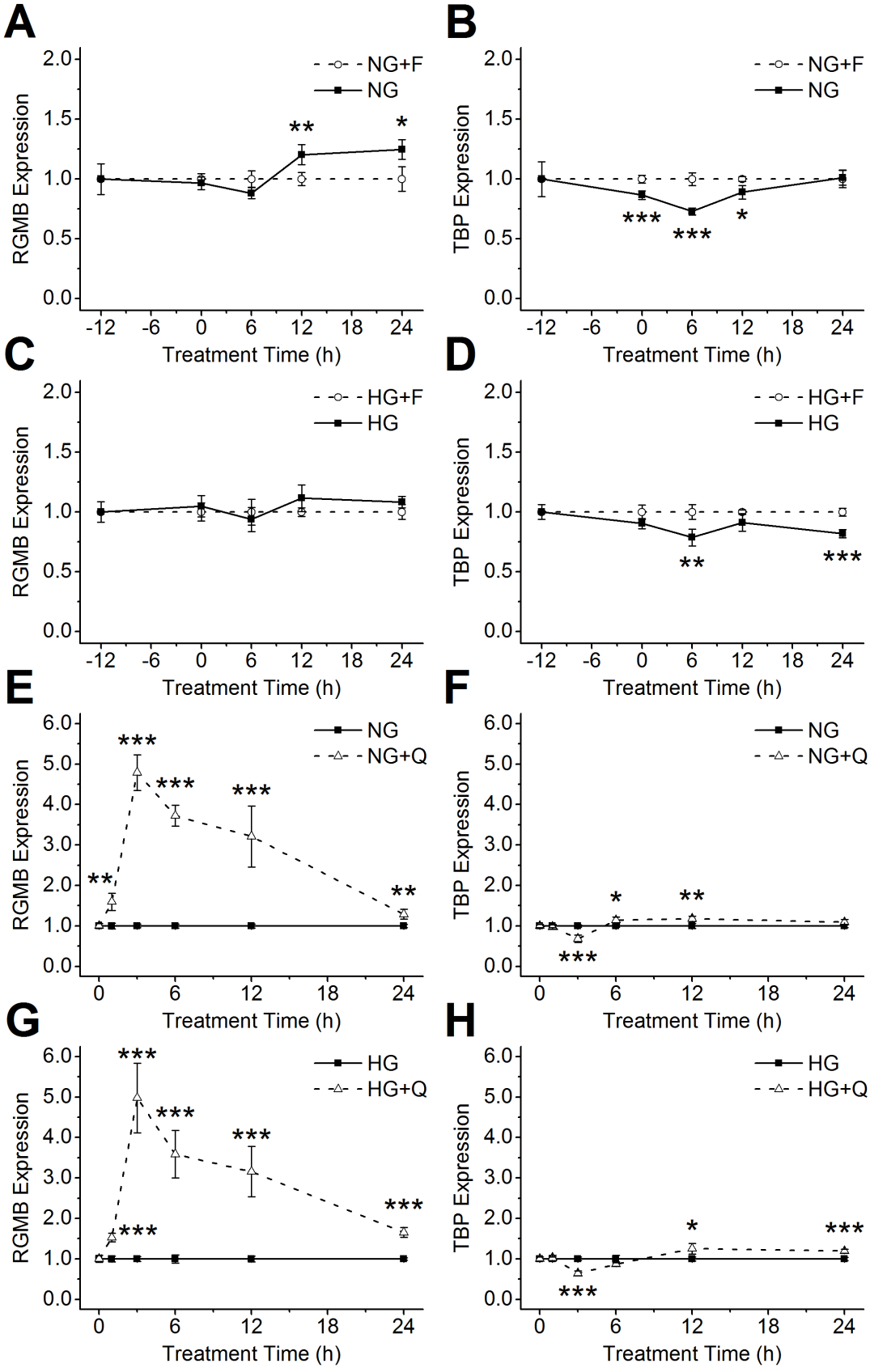

Fig. 9. RGMB and TBP mRNA expression in normal and high glucose-treated HepG2 cells. (A-D) Cells were seeded in normal (NG) or high (HG) glucose media and after 60 h (T = -12 h) the medium

was changed to medium ± FBS (F). Cells were treated at 72 h (T = 0 h) with ± FBS and lysates for RNA extraction were collected at 6, 12 and 24 h, with additional at -12 and 0 h. (E-H) Cells were grown in the same way and treated with serum-free medium from 60 h and with 20 µM quercetin (Q) at 72 h (T = 0 h) (or DMSO controls), and samples were collected at 1, 3, 6, 12 and 24 h. All data are mean values of fold-change in RGMB or TBP expression ± SEM (N/n = 6/18) vs respective controls. *$p < 0.05$, **$p < 0.01$, ***$p < 0.001$ vs respective control.

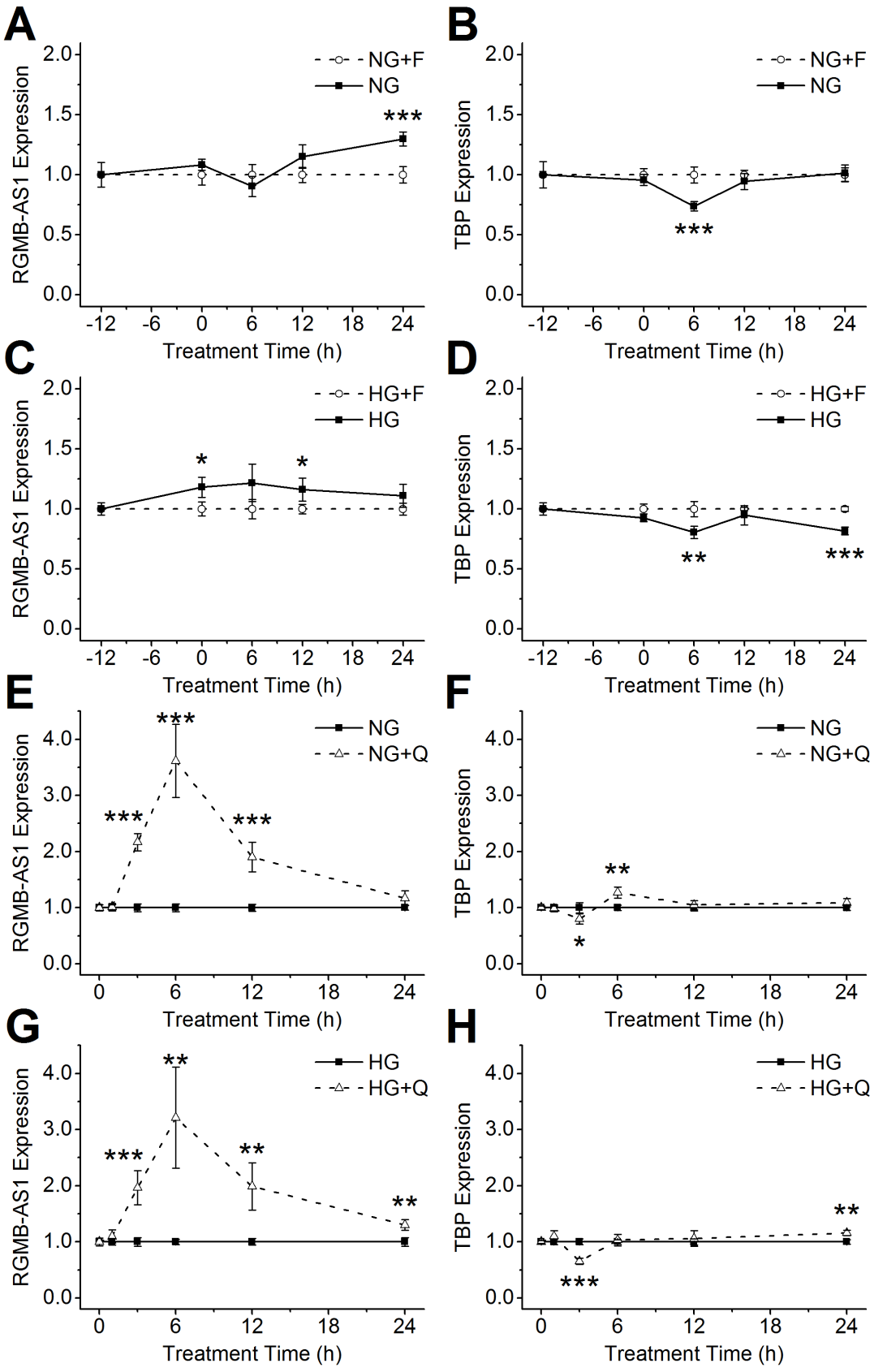

Fig. 10. RGMB-AS1 and TBP mRNA expression in normal and high glucose-treated HepG2 cells. (A-D) Cells were seeded in normal (NG) or high (HG) glucose media and after 60 h (T = -12 h) the

medium was changed to medium ± FBS (F). Cells were treated at 72 h (T = 0 h) with ± FBS and lysates for RNA extraction were collected at 6, 12 and 24 h, with additional at -12 and 0 h. (E-H) Cells were grown in the same way and treated with serum-free medium from 60 h and with 20 µM quercetin (Q) at 72 h (T = 0 h) (or DMSO controls), and samples were collected at 1, 3, 6, 12 and 24 h. All data are mean values of fold-change in RGMB-AS1 or TBP expression ± SEM (N/n = 6/18) vs respective controls. *$p < 0.05$, **$p < 0.01$, ***$p < 0.001$ vs respective control.

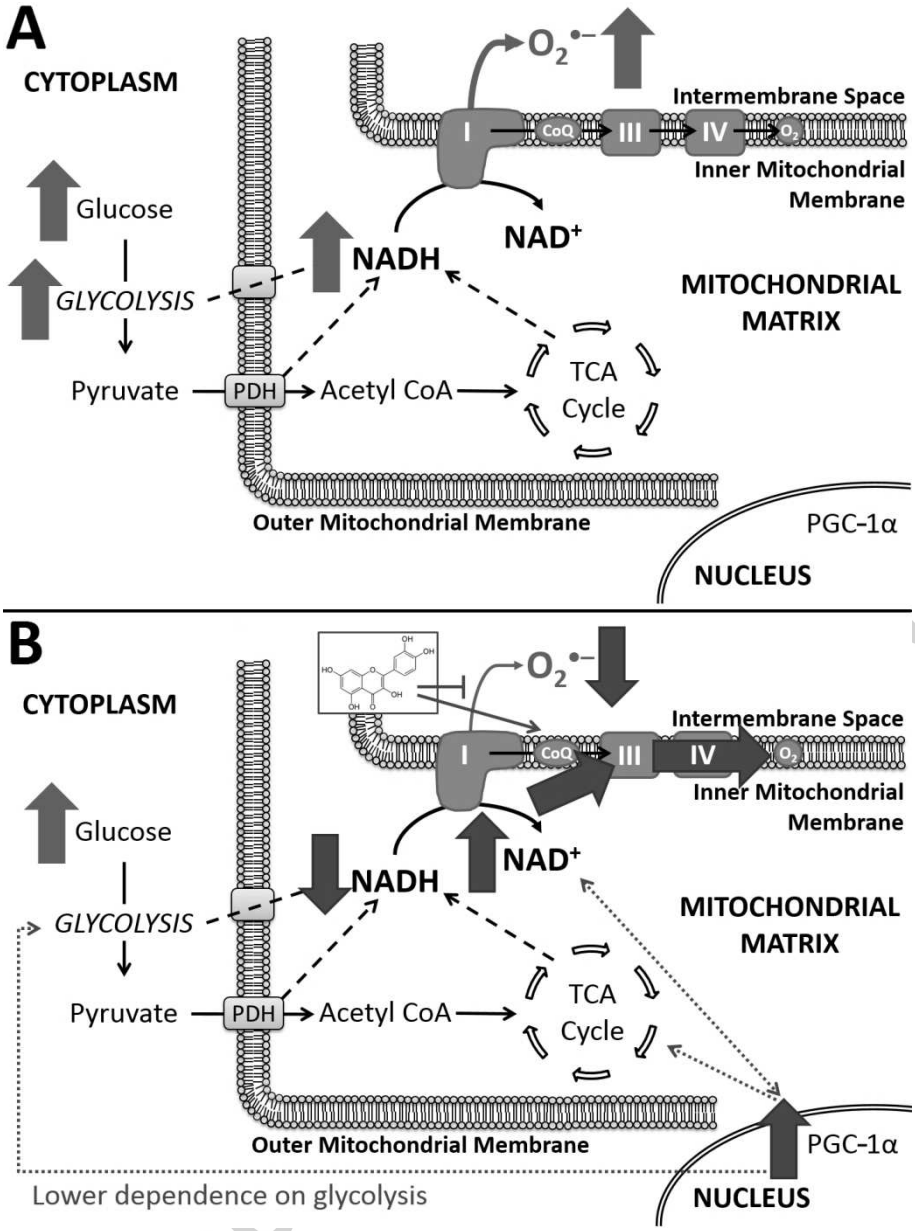

Fig. 11. Proposed mechanisms of action of quercetin in mitochondria in HepG2 cells treated chronically with high glucose. (A) Elevated glucose leads to increased NADH and overproduction of superoxide ($O_2^{\bullet-}$) at complex I of the electron transfer system. (B) Quercetin inhibits complex I at the coenzyme Q_{10}-binding site (CoQ), suppresses superoxide generation and attenuates the high glucose-induced proton leak across the inner mitochondrial membrane, while oxidising NADH and potentially allowing electron transfer to continue to complex III. This results in more efficient coupling with ATP synthesis. As a result, the NAD^+/NADH ratio is increased in parallel with induction of PGC-1α gene expression by quercetin; mitochondrial function is promoted and metabolic flux shifted to mitochondrial respiration, leading to lower oxidative stress and attenuation of high glucose-induced mitochondrial dysfunction, with increased net respiration and recovered complex I activity. RGMB and RGMB-AS1 (not shown) were increased with PGC-1α in correlation with the shift from

glycolysis. PDH – pyruvate dehydrogenase, TCA cycle – tricarboxylic cycle, Acetyl CoA – acetyl coenzyme A.

Discussion

High glucose-induced oxidative stress is linked to mitochondrial dysfunction, insulin resistance and metabolic syndrome [57]. Quercetin is thought to have a beneficial effect in various aspects of these metabolic diseases [20, 25, 31, 32, 58], either through restriction of ROS generation locally, or enhancement of cellular oxidative defences [34, 59-62]. Mechanisms of quercetin action have been reviewed [20] and it is apparent that information in the high glucose environment, and on longer term metabolic effects, remains limited.

Under conditions of chronic high glucose, serum starvation, or increased oxidative stress following treatment with H_2O_2, ETS complex I activity was decreased in agreement with previous reports [63, 64], while activity was increased by galactose, owing to increased oxidative phosphorylation fuelled by glutamine and fatty acids [65-68]. We show here that quercetin could dose-dependently protect against accumulating ROS and preserve the ETS protein complexes, potentially halting damage in mitochondrial DNA that ultimately occurs [4, 5, 8, 69]. We found that quercetin was able to relieve complex I from ROS-induced damage, especially under high glucose stress. Competitive inhibition of complex I at the CoQ-binding site was previously reported for quercetin [70] as well as a complementary activity as a CoQ mimetic, allowing electron transfer to continue from NADH to complex III [34, 35, 71]. Quercetin effects were time-dependent, probably due to quercetin metabolism, although sustained effects following 24 h after quercetin treatment point to metabolic changes. It has been shown that quercetin is almost fully metabolised within 4 h in HepG2 cells, while phase II metabolism was attenuated by high glucose [72]. We observed effects here even at 2.5 μM quercetin, although many of the mechanistic experiments were performed at 10 μM to ensure confidence in the results. Most previous publications cited in this paper have used much higher concentrations of quercetin. Ultimately, proof of any effect must be shown in vivo, but it is helpful to understand the mechanistic aspects using cultured cells.

A mild but significant decrease in citrate synthase activity was observed by quercetin treatment in both normal and high glucose while cell viability and plasma membrane integrity were improved. Since high glucose-induced loss of complex I activity was reversed with quercetin, this indicates improved mitochondrial function and increased oxidative capacity, limiting aberrant cell proliferation, a characteristic of glycolytic HepG2 cells. These results were also corroborated by increased RGMB and lncRNA RGMB-AS1 expression, which were previously correlated with decreased HepG2 proliferation and formation of a smaller number of colonies [40]. RGMb is also thought to reflect respiratory immunity in epithelial cells through binding to programmed death ligand 2 (PD-L2), while

blockade of the RGMB-PD-L2 interaction markedly impaired the development of respiratory tolerance [41]. Lowered mitochondrial content is likely owed to decreased lipogenesis and membrane formation, with pyruvate being directed to citrate and to oxidative metabolism rather than lipid anabolism; with increased oxidative function the mitochondrial population is streamlined.

Our hypothesis is also supported by lower proton leak across the IMM and an overall decrease in DCF fluorescence, albeit the latter is not exclusively indicative of ROS alone nor informative of specific ROS species formed [73], but limitations in this assay are outweighed by the highly significant differences observed in cells treated with quercetin and is the decrease is associated with the general change in redox status and lower oxidative stress. Previous studies have shown that quercetin improves mitochondrial bioenergetics in various other models [22, 23], while a role in maintaining membrane integrity has also been hypothesized [74-76]. The lower Leak in high glucose-treated cells with quercetin led to enhanced mitochondrial respiration by maximizing coupling efficiency and was reflected in higher Routine and net ETS respiration, indicative of increased use of ETS capacity for ATP turnover [54] as found here. These changes were only evident in the cells treated with 10 µM quercetin, while at 20 µM there was a decrease in routine respiration, consistent with the hypothesis that complex I may have been inhibited. Previous studies suggested that quercetin uncoupled ETS and oxidative phosphorylation while inhibiting mitochondrial respiration in isolated mitochondria [77-79]. In intact H9c2 rat cardiomyocytes short-term incubation with quercetin did not induce uncoupling, demonstrating that the effects seen in isolated mitochondria are attenuated in whole cells [80]. We provide supporting evidence for this here, as quercetin at high concentrations did not act as an uncoupler in HepG2 cells. When cells were not present, quercetin reacted with oxygen [81].

Importantly, the non-ETS residual oxygen consumption (ROX) was dose-dependently decreased by quercetin, which is indicative of less dependence on glycolysis. ROX represents the combined effect of oxygenase redox enzymes [54, 82, 83] and cell surface oxygen consumption via trans-plasma membrane electron transport (tPMET) [84]. Increased NADH oxidation by the actions of quercetin, as shown here by an increase in the NAD^+/NADH ratio, and via direct inhibition of ATPase enzymes [85-88] such as those involved in tPMET could explain our results. Lower dependence on glycolysis would be expected if more ATP is generated by quercetin-enhanced mitochondrial respiration and oxidation of alternative substrates such as glutamine and fatty acids [53], as shown here after 24 h.

Furthermore, quercetin inhibited glucose-6-phosphatase in insulin-resistant HepG2 cells and enhanced insulin sensitivity, allowing glycolysis to continue towards pyruvate [89]. We previously showed that 5 µM quercetin had a modest inhibitory effect on glucose uptake and metabolism in HepG2 cells over 12 h in normal glucose conditions [90]. However, HepG2 cells are known to be highly glycolytic with compromised oxidative phosphorylation, limited PI3K-Akt signalling and insulin responses [91]. A sustained decrease in ROS would potentially enhance insulin sensitivity in

cells in vivo, although this possibility is difficult to explore in immortalized cell models where glucose transport is mainly governed by GLUT1 and to a much lesser extent by insulin-responsive GLUT transporters.

A quercetin-induced increase in cellular NAD^+ could give rise to post-translational modifications through the AMPK-SIRT-PGC-1α axis, a central regulator of energy metabolism. PGC-1α has been linked to mitochondrial biogenesis and function while it is also activated under oxidative stress [92-94], and thought to suppresses transcription of glycolytic genes [95]. PGC-1α mRNA was increased in response to serum deprivation and further increased by quercetin under both normal and high glucose conditions, indicating that glucose concentration is not the critical effector in PGC-1α induction by quercetin. An increase in PGC-1α transcription corroborates the observed increase in NAD^+ in cells treated with quercetin, as NAD^+-dependent SIRT1 activates PGC-1α, which in turn promotes its own transcription [96, 97].

Given that quercetin was found to weakly enhance PGC-1α recruitment to PPARα, the main upstream nuclear factor regulating genes involved in mitochondrial energy metabolism, at concentrations achievable only in the cellular environment, we conclude that the effects of quercetin on PGC-1α are most likely via indirect mechanisms and a result of the effects seen on complex I and NADH as summarized in Fig. 11. However, we cannot exclude involvement of other transcription factors in the transcriptional regulation of PGC-1α by quercetin.

The protective effects of quercetin on mitochondrial bioenergetics in cells stressed by high glucose have not been demonstrated previously. Proteomics studies have revealed that complex I is lowered in diabetic patients [98], providing a potential target for the protective effects of quercetin against developing type 2 diabetes, as observed in epidemiological studies for quercetin-rich foods such as apples and tea [99, 100] and for quercetin in animal models of diabetes [101, 102]. The notable quercetin-induced increases in RGMB and RGMB-AS1 in HepG2 cells point towards a potential mechanism in the disruption of cancer cell proliferation [40], linked to the alteration from high dependence on glycolysis.

Acknowledgements

The research leading to these results has received funding from the European Research Council Advanced grant number 322467 (*'POLYTRUE?'*).

Author contributions

GW, AK and MH designed the study. MH optimised methods and carried out experiments; AK carried out the in vitro PGC-1α recruitment assay. AK and ST provided training and support for cell

culture, ProteinSimple and ddPCR analysis. JPB provided expertise and resources for respirometry experiments. MH wrote the first draft and all authors contributed to the final manuscript.

References

[1] Yan, L. J. Pathogenesis of chronic hyperglycemia: from reductive stress to oxidative stress. Journal of diabetes research **2014:**137919; 2014.

[2] Murphy, M. P. How mitochondria produce reactive oxygen species. The Biochemical journal **417:**1-13; 2009.

[3] Gero, D.; Torregrossa, R.; Perry, A.; Waters, A.; Le-Trionnaire, S.; Whatmore, J. L.; Wood, M.; Whiteman, M. The novel mitochondria-targeted hydrogen sulfide (H2S) donors AP123 and AP39 protect against hyperglycemic injury in microvascular endothelial cells in vitro. Pharmacological research **113:**186-198; 2016.

[4] Starkov, A. A. The role of mitochondria in reactive oxygen species metabolism and signaling. Annals of the New York Academy of Sciences **1147:**37-52; 2008.

[5] Kang, J.; Pervaiz, S. Mitochondria: redox metabolism and dysfunction. Biochemistry research international **2012:**896751; 2012.

[6] Evans, J. L.; Goldfine, I. D.; Maddux, B. A.; Grodsky, G. M. Oxidative stress and stress-activated signaling pathways: a unifying hypothesis of type 2 diabetes. Endocrine reviews **23:**599-622; 2002.

[7] Droge, W. Free radicals in the physiological control of cell function. Physiological reviews **82:**47-95; 2002.

[8] Hirst, J.; Roessler, M. M. Energy conversion, redox catalysis and generation of reactive oxygen species by respiratory complex I. Biochimica et biophysica acta **1857:**872-883; 2016.

[9] Brand, M. D. The sites and topology of mitochondrial superoxide production. Experimental gerontology **45:**466-472; 2010.

[10] Blake, R.; Trounce, I. A. Mitochondrial dysfunction and complications associated with diabetes. Biochimica et biophysica acta **1840:**1404-1412; 2014.

[11] Luo, X.; Li, R.; Yan, L. J. Roles of Pyruvate, NADH, and Mitochondrial Complex I in Redox Balance and Imbalance in beta Cell Function and Dysfunction. Journal of diabetes research **2015:**512618; 2015.

[12] Chow, J.; Rahman, J.; Achermann, J. C.; Dattani, M. T.; Rahman, S. Mitochondrial disease and endocrine dysfunction. Nature reviews. Endocrinology **13:**92-104; 2017.

[13] Zaccardi, F.; Webb, D. R.; Yates, T.; Davies, M. J. Pathophysiology of type 1 and type 2 diabetes mellitus: a 90-year perspective. Postgraduate medical journal **92:**63-69; 2016.

[14] Sivitz, W. I.; Yorek, M. A. Mitochondrial dysfunction in diabetes: from molecular mechanisms to functional significance and therapeutic opportunities. Antioxidants & redox signaling **12:**537-577; 2010.

[15] Montgomery, M. K.; Turner, N. Mitochondrial dysfunction and insulin resistance: an update. Endocrine connections **4:**R1-R15; 2015.

[16] Fiorani, M.; Guidarelli, A.; Blasa, M.; Azzolini, C.; Candiracci, M.; Piatti, E.; Cantoni, O. Mitochondria accumulate large amounts of quercetin: prevention of mitochondrial damage and release upon oxidation of the extramitochondrial fraction of the flavonoid. The Journal of nutritional biochemistry **21:**397-404; 2010.

[17] Ishisaka, A.; Kawabata, K.; Miki, S.; Shiba, Y.; Minekawa, S.; Nishikawa, T.; Mukai, R.; Terao, J.; Kawai, Y. Mitochondrial dysfunction leads to deconjugation of quercetin glucuronides in inflammatory macrophages. PloS one **8:**e80843; 2013.

[18] Galindo, P.; Rodriguez-Gómez, I.; González-Manzano, S.; Dueñas, M.; Jiménez, R.; Menéndez, C.; Vargas, F.; Tamargo, J.; Santos-Buelga, C.; Pérez-Vizcaíno, F.; Duarte, J. Glucuronidated Quercetin Lowers Blood Pressure in Spontaneously Hypertensive Rats via Deconjugation. PloS one **7:**e32673; 2012.

[19] Menendez, C.; Duenas, M.; Galindo, P.; Gonzalez-Manzano, S.; Jimenez, R.; Moreno, L.; Zarzuelo, M. J.; Rodriguez-Gomez, I.; Duarte, J.; Santos-Buelga, C.; Perez-Vizcaino, F. Vascular deconjugation of quercetin glucuronide: the flavonoid paradox revealed? Molecular nutrition & food research **55:**1780-1790; 2011.

[20] de Oliveira, M. R.; Nabavi, S. M.; Braidy, N.; Setzer, W. N.; Ahmed, T.; Nabavi, S. F. Quercetin and the mitochondria: A mechanistic view. Biotechnology advances **34:**532-549; 2016.

[21] Sandoval-Acuna, C.; Ferreira, J.; Speisky, H. Polyphenols and mitochondria: an update on their increasingly emerging ROS-scavenging independent actions. Archives of biochemistry and biophysics **559:**75-90; 2014.

[22] Carrasco-Pozo, C.; Tan, K. N.; Reyes-Farias, M.; De La Jara, N.; Ngo, S. T.; Garcia-Diaz, D. F.; Llanos, P.; Cires, M. J.; Borges, K. The deleterious effect of cholesterol and protection by quercetin on mitochondrial bioenergetics of pancreatic beta-cells, glycemic control and inflammation: In vitro and in vivo studies. Redox biology **9:**229-243; 2016.

[23] Nichols, M.; Zhang, J.; Polster, B. M.; Elustondo, P. A.; Thirumaran, A.; Pavlov, E. V.; Robertson, G. S. Synergistic neuroprotection by epicatechin and quercetin: Activation of convergent mitochondrial signaling pathways. Neuroscience **308:**75-94; 2015.

[24] Rayamajhi, N.; Kim, S. K.; Go, H.; Joe, Y.; Callaway, Z.; Kang, J. G.; Ryter, S. W.; Chung, H. T. Quercetin induces mitochondrial biogenesis through activation of HO-1 in HepG2 cells. Oxidative medicine and cellular longevity **2013:**154279; 2013.

[25] Kim, C. S.; Kwon, Y.; Choe, S. Y.; Hong, S. M.; Yoo, H.; Goto, T.; Kawada, T.; Choi, H. S.; Joe, Y.; Chung, H. T.; Yu, R. Quercetin reduces obesity-induced hepatosteatosis by enhancing mitochondrial oxidative metabolism via heme oxygenase-1. Nutrition & metabolism **12:**33; 2015.

[26] Nyambe-Silavwe, H.; Villa-Rodriguez, J. A.; Ifie, I.; Holmes, M.; Aydin, E.; Jensen, J. M.; Williamson, G. Inhibition of human α-amylase by dietary polyphenols. J Funct Foods **19, Part A:**723-732; 2015.

[27] Williamson, G. Possible effects of dietary polyphenols on sugar absorption and digestion. Molecular nutrition & food research **57:**48-57; 2013.

[28] Nomura, M.; Takahashi, T.; Nagata, N.; Tsutsumi, K.; Kobayashi, S.; Akiba, T.; Yokogawa, K.; Moritani, S.; Miyamoto, K. Inhibitory mechanisms of flavonoids on insulin-stimulated glucose uptake in MC3T3-G2/PA6 adipose cells. Biological & pharmaceutical bulletin **31:**1403-1409; 2008.

[29] Leiherer, A.; Stoemmer, K.; Muendlein, A.; Saely, C. H.; Kinz, E.; Brandtner, E. M.; Fraunberger, P.; Drexel, H. Quercetin Impacts Expression of Metabolism- and Obesity-Associated Genes in SGBS Adipocytes. Nutrients **8**; 2016.

[30] Vessal, M.; Hemmati, M.; Vasei, M. Antidiabetic effects of quercetin in streptozocin-induced diabetic rats. Comparative biochemistry and physiology. Toxicology & pharmacology : CBP **135C:**357-364; 2003.

[31] Chis, I. C.; Muresan, A.; Oros, A.; Nagy, A. L.; Clichici, S. Protective effects of Quercetin and chronic moderate exercise (training) against oxidative stress in the liver tissue of streptozotocin-induced diabetic rats. Acta physiologica Hungarica **103:**49-64; 2016.

[32] Eid, H. M.; Haddad, P. S. The Antidiabetic Potential of Quercetin: Underlying Mechanisms. Current medicinal chemistry **24:**355-364; 2017.

[33] Akash, M. S.; Rehman, K.; Chen, S. Spice plant Allium cepa: dietary supplement for treatment of type 2 diabetes mellitus. Nutrition (Burbank, Los Angeles County, Calif.) **30:**1128-1137; 2014.

[34] Lagoa, R.; Graziani, I.; Lopez-Sanchez, C.; Garcia-Martinez, V.; Gutierrez-Merino, C. Complex I and cytochrome c are molecular targets of flavonoids that inhibit hydrogen peroxide production by mitochondria. Biochimica et biophysica acta **1807:**1562-1572; 2011.

[35] Sandoval-Acuna, C.; Lopez-Alarcon, C.; Aliaga, M. E.; Speisky, H. Inhibition of mitochondrial complex I by various non-steroidal anti-inflammatory drugs and its protection by quercetin via a coenzyme Q-like action. Chemico-biological interactions **199:**18-28; 2012.

[36] Waseem, M.; Parvez, S. Neuroprotective activities of curcumin and quercetin with potential relevance to mitochondrial dysfunction induced by oxaliplatin. Protoplasma **253:**417-430; 2016.

[37] Siebold, C.; Yamashita, T.; Monnier, P. P.; Mueller, B. K.; Pasterkamp, R. J. RGMs: Structural Insights, Molecular Regulation, and Downstream Signaling. Trends in cell biology **27:**365-378; 2017.

[38] Li, P.; Li, J.; Yang, R.; Zhang, F.; Wang, H.; Chu, H.; Lu, Y.; Dun, S.; Wang, Y.; Zang, W.; Du, Y.; Chen, X.; Zhao, G.; Zhang, G. Study on expression of lncRNA RGMB-AS1 and repulsive guidance molecule b in non-small cell lung cancer. Diagnostic pathology **10:**63; 2015.

[39] Shi, Y.; Chen, G. B.; Huang, X. X.; Xiao, C. X.; Wang, H. H.; Li, Y. S.; Zhang, J. F.; Li, S.; Xia, Y.; Ren, J. L.; Guleng, B. Dragon (repulsive guidance molecule b, RGMb) is a novel gene that promotes colorectal cancer growth. Oncotarget **6:**20540-20554; 2015.

[40] Sheng, N.; Li, Y.; Qian, R.; Li, Y. The clinical significance and biological function of lncRNA RGMB-AS1 in hepatocellular carcinoma. Biomedicine & pharmacotherapy = Biomedecine & pharmacotherapie **98:**577-584; 2018.

[41] Xiao, Y.; Yu, S.; Zhu, B.; Bedoret, D.; Bu, X.; Francisco, L. M.; Hua, P.; Duke-Cohan, J. S.; Umetsu, D. T.; Sharpe, A. H.; DeKruyff, R. H.; Freeman, G. J. RGMb is a novel binding partner for

PD-L2 and its engagement with PD-L2 promotes respiratory tolerance. The Journal of experimental medicine **211:**943-959; 2014.

[42] Wong, C. C.; Botting, N. P.; Orfila, C.; Al-Maharik, N.; Williamson, G. Flavonoid conjugates interact with organic anion transporters (OATs) and attenuate cytotoxicity of adefovir mediated by organic anion transporter 1 (OAT1/SLC22A6). Biochemical pharmacology **81:**942-949; 2011.

[43] Spinazzi, M.; Casarin, A.; Pertegato, V.; Salviati, L.; Angelini, C. Assessment of mitochondrial respiratory chain enzymatic activities on tissues and cultured cells. Nature protocols **7:**1235-1246; 2012.

[44] Usta, J.; Kreydiyyeh, S.; Knio, K.; Barnabe, P.; Bou-Moughlabay, Y.; Dagher, S. Linalool decreases HepG2 viability by inhibiting mitochondrial complexes I and II, increasing reactive oxygen species and decreasing ATP and GSH levels. Chemico-biological interactions **180:**39-46; 2009.

[45] Ragan, C. I., Wilson, M.T., Darley-Usmar, V.M., Lowe, P.N. Ch. 4: Sub-fractionation of mitochondria and isolation of the proteins of oxidative phosphorylation. In: Darley-Usmar, V. M., Rickwood, D., Wilson, M.T., ed. Mitochondria a practical approach: IRL Press; 1987.

[46] Janssen, A. J.; Trijbels, F. J.; Sengers, R. C.; Smeitink, J. A.; van den Heuvel, L. P.; Wintjes, L. T.; Stoltenborg-Hogenkamp, B. J.; Rodenburg, R. J. Spectrophotometric assay for complex I of the respiratory chain in tissue samples and cultured fibroblasts. Clinical chemistry **53:**729-734; 2007.

[47] de Wit, L. E.; Scholte, H. R.; Sluiter, W. Correct assay of complex I activity in human skin fibroblasts by timely addition of rotenone. Clinical chemistry **54:**1921-1922; author reply 1922-1924; 2008.

[48] Oliveira, K. K.; Kiyomoto, B. H.; Rodrigues Ade, S.; Tengan, C. H. Complex I spectrophotometric assay in cultured cells: detailed analysis of key factors. Analytical biochemistry **435:**57-59; 2013.

[49] Wang, H.; Joseph, J. A. Quantifying cellular oxidative stress by dichlorofluorescein assay using microplate reader. Free radical biology & medicine **27:**612-616; 1999.

[50] Ernst, O.; Zor, T. Linearization of the bradford protein assay. Journal of visualized experiments : JoVE **38:**1918; 2010.

[51] Bradford, M. M. A rapid and sensitive method for the quantitation of microgram quantities of protein utilizing the principle of protein-dye binding. Analytical biochemistry **72:**248-254; 1976.

[52] Larsen, S.; Nielsen, J.; Hansen, C. N.; Nielsen, L. B.; Wibrand, F.; Stride, N.; Schroder, H. D.; Boushel, R.; Helge, J. W.; Dela, F.; Hey-Mogensen, M. Biomarkers of mitochondrial content in skeletal muscle of healthy young human subjects. The Journal of physiology **590:**3349-3360; 2012.

[53] Gnaiger, E. Mitochondrial pathways and respiratory control. An introduction to OXPHOS analysis. Innsbruck: OROBOROS MiPNet Publications; 2014.

[54] Brand, M. D.; Nicholls, D. G. Assessing mitochondrial dysfunction in cells. The Biochemical journal **435:**297-312; 2011.

[55] Tumova, S.; Kerimi, A.; Porter, K. E.; Williamson, G. Transendothelial glucose transport is not restricted by extracellular hyperglycaemia. Vascular pharmacology **87:**219-229; 2016.

[56] Zhang, J. H.; Chung, T. D.; Oldenburg, K. R. A Simple Statistical Parameter for Use in Evaluation and Validation of High Throughput Screening Assays. Journal of biomolecular screening **4:**67-73; 1999.

[57] Yang, H.; Jin, X.; Kei Lam, C. W.; Yan, S. K. Oxidative stress and diabetes mellitus. Clinical chemistry and laboratory medicine : CCLM / FESCC **49:**1773-1782; 2011.

[58] Eid, H. M.; Martineau, L. C.; Saleem, A.; Muhammad, A.; Vallerand, D.; Benhaddou-Andaloussi, A.; Nistor, L.; Afshar, A.; Arnason, J. T.; Haddad, P. S. Stimulation of AMP-activated protein kinase and enhancement of basal glucose uptake in muscle cells by quercetin and quercetin glycosides, active principles of the antidiabetic medicinal plant Vaccinium vitis-idaea. Molecular nutrition & food research **54:**991-1003; 2010.

[59] Vargas, A. J.; Burd, R. Hormesis and synergy: pathways and mechanisms of quercetin in cancer prevention and management. Nutrition reviews **68:**418-428; 2010.

[60] Ji, L. L.; Sheng, Y. C.; Zheng, Z. Y.; Shi, L.; Wang, Z. T. The involvement of p62-Keap1-Nrf2 antioxidative signaling pathway and JNK in the protection of natural flavonoid quercetin against hepatotoxicity. Free radical biology & medicine **85:**12-23; 2015.

[61] Moskaug, J. O.; Carlsen, H.; Myhrstad, M. C.; Blomhoff, R. Polyphenols and glutathione synthesis regulation. The American journal of clinical nutrition **81:**277S-283S; 2005.

[62] Jimenez, R.; Lopez-Sepulveda, R.; Romero, M.; Toral, M.; Cogolludo, A.; Perez-Vizcaino, F.; Duarte, J. Quercetin and its metabolites inhibit the membrane NADPH oxidase activity in vascular smooth muscle cells from normotensive and spontaneously hypertensive rats. Food & function **6:**409-414; 2015.

[63] Jiang, J.; Yu, S.; Jiang, Z.; Liang, C.; Yu, W.; Li, J.; Du, X.; Wang, H.; Gao, X.; Wang, X. N-acetyl-serotonin protects HepG2 cells from oxidative stress injury induced by hydrogen peroxide. Oxidative medicine and cellular longevity **2014:**310504; 2014.

[64] Takeda, T.; Akao, M.; Matsumoto-Ida, M.; Kato, M.; Takenaka, H.; Kihara, Y.; Kume, T.; Akaike, A.; Kita, T. Serofendic acid, a novel substance extracted from fetal calf serum, protects against oxidative stress in neonatal rat cardiac myocytes. Journal of the American College of Cardiology **47:**1882-1890; 2006.

[65] Reitzer, L. J.; Wice, B. M.; Kennell, D. Evidence that glutamine, not sugar, is the major energy source for cultured HeLa cells. The Journal of biological chemistry **254:**2669-2676; 1979.

[66] Robinson, B. H.; Petrova-Benedict, R.; Buncic, J. R.; Wallace, D. C. Nonviability of cells with oxidative defects in galactose medium: a screening test for affected patient fibroblasts. Biochemical medicine and metabolic biology **48:**122-126; 1992.

[67] Marroquin, L. D.; Hynes, J.; Dykens, J. A.; Jamieson, J. D.; Will, Y. Circumventing the Crabtree effect: replacing media glucose with galactose increases susceptibility of HepG2 cells to mitochondrial toxicants. Toxicological sciences : an official journal of the Society of Toxicology **97:**539-547; 2007.

[68] Andrzejewski, S.; Gravel, S. P.; Pollak, M.; St-Pierre, J. Metformin directly acts on mitochondria to alter cellular bioenergetics. Cancer & metabolism **2:**12; 2014.

[69] Guo, C.; Sun, L.; Chen, X.; Zhang, D. Oxidative stress, mitochondrial damage and neurodegenerative diseases. Neural regeneration research **8:**2003-2014; 2013.

[70] Carrasco-Pozo, C.; Mizgier, M. L.; Speisky, H.; Gotteland, M. Differential protective effects of quercetin, resveratrol, rutin and epigallocatechin gallate against mitochondrial dysfunction induced by indomethacin in Caco-2 cells. Chemico-biological interactions **195:**199-205; 2012.

[71] Hodnick, W. F.; Bohmont, C. W.; Capps, C.; Pardini, R. S. Inhibition of the mitochondrial NADH-oxidase (NADH-coenzyme Q oxido-reductase) enzyme system by flavonoids: a structure-activity study. Biochemical pharmacology **36:**2873-2874; 1987.

[72] Hashimoto, N.; Blumberg, J. B.; Chen, C. Y. Hyperglycemia and Anthocyanin Inhibit Quercetin Metabolism in HepG2 Cells. Journal of medicinal food **19:**141-147; 2016.

[73] Hardy, M.; Zielonka, J.; Karoui, H.; Sikora, A.; Michalski, R.; Podsiadly, R.; Lopez, M.; Vasquez-Vivar, J.; Kalyanaraman, B.; Ouari, O. Detection and Characterization of Reactive Oxygen

and Nitrogen Species in Biological Systems by Monitoring Species-Specific Products. Antioxidants & redox signaling **28:**1416-1432; 2018.

[74] Sanver, D.; Murray, B. S.; Sadeghpour, A.; Rappolt, M.; Nelson, A. L. Experimental Modeling of Flavonoid-Biomembrane Interactions. Langmuir : the ACS journal of surfaces and colloids **32:**13234-13243; 2016.

[75] Modriansky, M.; Gabrielova, E. Uncouple my heart: the benefits of inefficiency. Journal of bioenergetics and biomembranes **41:**133-136; 2009.

[76] Margina, D.; Gradinaru, D.; Manda, G.; Neagoe, I.; Ilie, M. Membranar effects exerted in vitro by polyphenols - quercetin, epigallocatechin gallate and curcumin - on HUVEC and Jurkat cells, relevant for diabetes mellitus. Food and chemical toxicology : an international journal published for the British Industrial Biological Research Association **61:**86-93; 2013.

[77] Ortega, R.; Garcia, N. The flavonoid quercetin induces changes in mitochondrial permeability by inhibiting adenine nucleotide translocase. Journal of bioenergetics and biomembranes **41:**41-47; 2009.

[78] Dorta, D. J.; Pigoso, A. A.; Mingatto, F. E.; Rodrigues, T.; Prado, I. M.; Helena, A. F.; Uyemura, S. A.; Santos, A. C.; Curti, C. The interaction of flavonoids with mitochondria: effects on energetic processes. Chemico-biological interactions **152:**67-78; 2005.

[79] Trumbeckaite, S.; Bernatoniene, J.; Majiene, D.; Jakstas, V.; Savickas, A.; Toleikis, A. The effect of flavonoids on rat heart mitochondrial function. Biomedicine & pharmacotherapy = Biomedecine & pharmacotherapie **60:**245-248; 2006.

[80] V. Zholobenko, A.; Mouithys-Mickalad, A.; Dostal, Z.; Serteyn, D.; Modrianský, M. On the causes and consequences of the uncoupler-like effects of quercetin and dehydrosilybin in H9c2 cells. **12:**e0185691; 2017.

[81] Morales, J.; Günther, G.; Zanocco, A. L.; Lemp, E. Singlet Oxygen Reactions with Flavonoids. A Theoretical – Experimental Study. PloS one **7:**e40548; 2012.

[82] Banh, R. S.; Iorio, C.; Marcotte, R.; Xu, Y.; Cojocari, D.; Rahman, A. A.; Pawling, J.; Zhang, W.; Sinha, A.; Rose, C. M.; Isasa, M.; Zhang, S.; Wu, R.; Virtanen, C.; Hitomi, T.; Habu, T.; Sidhu, S. S.; Koizumi, A.; Wilkins, S. E.; Kislinger, T.; Gygi, S. P.; Schofield, C. J.; Dennis, J. W.; Wouters, B. G.; Neel, B. G. PTP1B controls non-mitochondrial oxygen consumption by regulating RNF213 to promote tumour survival during hypoxia. Nature cell biology **18:**803-813; 2016.

[83] Kerimi, A.; Williamson, G. At the interface of antioxidant signalling and cellular function: Key polyphenol effects. Molecular nutrition & food research **60:**1770-1788; 2016.

[84] Herst, P. M.; Berridge, M. V. Cell surface oxygen consumption: a major contributor to cellular oxygen consumption in glycolytic cancer cell lines. Biochimica et biophysica acta **1767:**170-177; 2007.

[85] Gasparin, F. R.; Salgueiro-Pagadigorria, C. L.; Bracht, L.; Ishii-Iwamoto, E. L.; Bracht, A.; Constantin, J. Action of quercetin on glycogen catabolism in the rat liver. Xenobiotica; the fate of foreign compounds in biological systems **33:**587-602; 2003.

[86] Racker, E. Effect of quercetin on ATP-driven pumps and glycolysis. Progress in clinical and biological research **213:**257-271; 1986.

[87] Davis, F. B.; Middleton, E., Jr.; Davis, P. J.; Blas, S. D. Inhibition by quercetin of thyroid hormone stimulation in vitro of human red blood cell Ca2+-ATPase activity. Cell calcium **4:**71-81; 1983.

[88] Lang, D. R.; Racker, E. Effects of quercetin and F1 inhibitor on mitochondrial ATPase and energy-linked reactions in submitochondrial particles. Biochimica et biophysica acta **333:**180-186; 1974.

[89] Teng, H.; Chen, L.; Song, H. The potential beneficial effects of phenolic compounds isolated from A. pilosa Ledeb on insulin-resistant hepatic HepG2 cells. Food & function **7:**4400-4409; 2016.

[90] Kerimi, A.; Jailani, F.; Williamson, G. Modulation of cellular glucose metabolism in human HepG2 cells by combinations of structurally related flavonoids. Molecular nutrition & food research **59:**894-906; 2015.

[91] Kerimi, A.; Williamson, G. Differential Impact of Flavonoids on Redox Modulation, Bioenergetics, and Cell Signaling in Normal and Tumor Cells: A Comprehensive Review. Antioxidants & redox signaling**:** [Epub ahead of print] https://doi.org/10.1089/ars.2017.7086; 2017.

[92] Tang, B. L. Sirt1 and the Mitochondria. Molecules and cells **39:**87-95; 2016.

[93] Austin, S.; St-Pierre, J. PGC1alpha and mitochondrial metabolism--emerging concepts and relevance in ageing and neurodegenerative disorders. Journal of cell science **125:**4963-4971; 2012.

[94] Canto, C.; Gerhart-Hines, Z.; Feige, J. N.; Lagouge, M.; Noriega, L.; Milne, J. C.; Elliott, P. J.; Puigserver, P.; Auwerx, J. AMPK regulates energy expenditure by modulating NAD+ metabolism and SIRT1 activity. Nature **458:**1056-1060; 2009.

[95] Rodgers, J. T.; Lerin, C.; Haas, W.; Gygi, S. P.; Spiegelman, B. M.; Puigserver, P. Nutrient control of glucose homeostasis through a complex of PGC-1alpha and SIRT1. Nature **434:**113-118; 2005.

[96] Sugden, M. C.; Holness, M. J. Metformin, metabolic stress, and mitochondria. Focus on "A novel inverse relationship between metformin-triggered AMPK-SIRT1 signaling and p53 protein abundance in high glucose-exposed HepG2 cells". American journal of physiology. Cell physiology **303:**C1-3; 2012.

[97] Nelson, L. E.; Valentine, R. J.; Cacicedo, J. M.; Gauthier, M. S.; Ido, Y.; Ruderman, N. B. A novel inverse relationship between metformin-triggered AMPK-SIRT1 signaling and p53 protein abundance in high glucose-exposed HepG2 cells. American journal of physiology. Cell physiology **303:**C4-C13; 2012.

[98] Peinado, J. R.; Diaz-Ruiz, A.; Fruhbeck, G.; Malagon, M. M. Mitochondria in metabolic disease: getting clues from proteomic studies. Proteomics **14:**452-466; 2014.

[99] Yang, J.; Mao, Q. X.; Xu, H. X.; Ma, X.; Zeng, C. Y. Tea consumption and risk of type 2 diabetes mellitus: a systematic review and meta-analysis update. BMJ Open **4:**e005632; 2014.

[100] Guo, X. F.; Yang, B.; Tang, J.; Jiang, J. J.; Li, D. Apple and pear consumption and type 2 diabetes mellitus risk: a meta-analysis of prospective cohort studies. Food Funct **8:**927-934; 2017.

[101] Mahmoud, M. F.; Hassan, N. A.; El Bassossy, H. M.; Fahmy, A. Quercetin protects against diabetes-induced exaggerated vasoconstriction in rats: effect on low grade inflammation. PLoS One **8:**e63784; 2013.

[102] Elbe, H.; Esrefoglu, M.; Vardi, N.; Taslidere, E.; Ozerol, E.; Tanbek, K. Melatonin, quercetin and resveratrol attenuates oxidative hepatocellular injury in streptozotocin-induced diabetic rats. Hum Exp Toxicol **34:**859-868; 2015.

Highlights:

- Quercetin protects mitochondrial function from high glucose-induced stress
- Through an increase in repulsive guidance molecule b (RGMB) mRNA and its long non-coding RNA, quercetin may initiate a change of the glycolytic phenotype of HepG2 cells.
- Quercetin reversed chronic high glucose-induced oxidative stress and mitochondrial dysfunction
- Quercetin induced lower ROS in combination with improved complex I activity and ETS coupling efficiency